Structural Insights Into Heavy Chalcogen Polycations and Their Stabilization via (Hydrogen)polysulfates.

Jan Langwald,[a] Sergi Burguera,[b] Antonio Frontera [*b] and Mathias S. Wickleder[*a]

[a] *Institute of Inorganic and Materials Chemistry, University of Cologne, Greinstr. 6, 50939 Cologne, Germany. E-mail: mathias.wickleder@uni-koeln.de*
[b] *Universitat de les Illes Balears, Crta de Valldemossa km 7.5, 07122 Palma de Mallorca, Baleares, Spain. E-mail: toni.frontera@uib.es*

Table of Contents

A. Synthesis

General Procedure

SO_3 was obtained in a specially designed apparatus for the generation, distillation and subsequent transfer into glass ampoules under nitrogen gas. For this purpose, fuming sulfuric acid (65% SO_3, used as received, Merck, Darmstadt, Germany) was added via a dropping funnel into a 500 mL flask with P_4O_{10} (250 g, >97%, Merck, Darmstadt) with a dosage rate of 1 mL / minute. At the same time, the flask was heated at 130 °C and the generated SO_3 distilled into a connected burette body (scaling 0.01 ml). A connected glass ampoule (l = 200 mm, $ø$ = 16 mm, thickness of the tube wall = 1.80 mm) containing the solid starting materials was then filled with the required amount of SO_3.

1,2-Dichloroethane was refluxed with P_4O_{10} for ~5 h, followed by distillation and storage over molecular sieves (4 Å) prior to use. Selenoyl chloride ($SeOCl_2$) was prepared according to literature procedures and it's purity confirmed *via* ^{77}Se NMR spectroscopy ([$CDCl_3$]:1496 ppm, s).[1-2]

Synthesis of $[Se_4][HS_2O_7]_2$ (1)

Compound **1** was previously isolated and reported by Gillespie in the space group $P2_1/c$.[3] We herein report two additional preparative routes yielding large amounts of crystalline material. We revisited the compound for improved data quality and subsequent quantum chemical calculations. We used the nowadays more common space group $P2_1/n$ (transformation matrix: 1 0 -1; 0 -1 0; 0 0 -1).

165.4 mg (2.09 mmol, 1.00 eq.) of Selenium powder (99+%, ACROS Organics) and 0.12 mL (1.80 mmol, 0.86 eq.) of Chlorosulfuric acid (97%, Thermo Scientific) were filled into a preheated glass ampoule (3.3 borosilicate). 0.20 mL SO_3 (5.00 mmol, 2.39 eq.) were condensed on top and the ampoule was sealed under reduced pressure ($1{\cdot}10^{-3}$ mbar) with a gas burner. The reaction vessel was heated to 80 °C within 24 h, dwelled at this temperature for 48 h and cooled down to room temperature (in the following 'r.t.') within 90 h. After cooling, bright orange crystals could be isolated from the mother liquor. The conversion is quantitative.

Product **1** could also be isolated after the reaction of 162.0 mg (2.05 mmol, 1.00 eq.) Selenium powder with 0.10 mL (1.27 mmol, 0.62 eq.) of 1,2-Dichloroethane and 0.20 mL SO_3 (5.00 mmol, 2.44 eq.).

Synthesis of $[Se_4][S_2O_7]$ (2)

204.4 mg (0.98 mmol, 1.00 eq.) of elemental Bismuth (99.5%, Alfa Aesar) and 0.20 mL (2.93 mmol, 2.99 eq.) of $SeOCl_2$ were filled into a preheated glass ampoule (3.3 borosilicate). 0.20 mL SO_3 (5.00 mmol, 5.11 eq.) were condensed on top and the ampoule was sealed under reduced pressure ($1{\cdot}10^{-3}$ mbar) with a gas burner. . The reaction vessel was heated to 80 °C within 24 h, dwelled at this temperature for 6 h and cooled down to r.t. within 90 h. After cooling, bright orange crystals could be isolated as a byproduct from the high-viscous mother liquor. The main product $[SeCl_3][Bi(S_2O_7)_2]$ will be reported separately.[4]

Synthesis of $[Se_4][HS_3O_{10}]_2$ (3)

80.6 mg (1.02 mmol, 1.00 eq.) of Selenium powder (99+%, ACROS Organics) and 0.12 mL (1.80 mmol, 1.76 eq.) of Chlorosulfuric acid (97%, Thermo Scientific) were filled into a preheated glass ampoule (3.3 borosilicate). 0.20 mL SO_3 (5.00 mmol, 4.90 eq.) were condensed on top and the ampoule was sealed under reduced pressure ($1{\cdot}10^{-3}$ mbar) with a gas burner. The resulting dark-green solution was stored at -20 °C. Within a period of 3 weeks, the solution turned yellow and bright yellow crystals grew from the mother liquid.

Synthesis of $[Te_4][HS_3O_{10}]_2$ (3), $[Te_6][HS_3O_{10}]_4$ (4), $[Te_6][HS_3O_{10}]_4$–I (5) and $[Te_6][HS_3O_{10}]_4$–II

131.5 mg (1.03 mmol, 1.00 eq.) of Tellurium powder (99.80%, ACROS Organics) and 0.12 mL (1.80 mmol, 1.75 eq.) of Chlorosulfuric acid (97%, Thermo Scientific) were filled into a preheated glass ampoule (3.3 borosilicate). 0.20 mL SO_3 (5.00 mmol, 4.90 eq.) were condensed on top and the ampoule was sealed under reduced pressure ($1 \cdot 10^{-3}$ mbar) with a gas burner. The resulting berry-red solution was stored at 7 °C. After 24 h, colourless and red crystals grew from the mother liquid. The red single crystals were identified as product **3**, whereby the colourless crystals could be identified as products **4** and **5** + **6**, respectively. They can only be differentiated by small variations in the crystal morphology.

Synthesis of $[Te_6][S_4O_{13}]_2$ (7)

128.6 mg (1.01 mmol, 1.00 eq.) of Tellurium powder (99.80%, ACROS Organics) and 0.30 mL (4.13 mmol, 4.09 eq.) of SO_2Cl_2 (Sigma-Aldrich) were filled into a preheated glass ampoule (3.3 borosilicate). 0.60 mL SO_3 (15.00 mmol, 14.85 eq.) were condensed on top and the ampoule was sealed under reduced pressure ($1 \cdot 10^{-3}$ mbar) with a gas burner. The resulting solution was stored at 7 °C. After 24 h, slightly yellow crystals and colorless crystals grew from the mother liquid. The yellow single crystals were identified as product **7**, whereby the colourless crystals could be identified $Te[S_2O_7]_2$.[5]

B. Structure Determination and Crystallographic Details

General Procedure

The single crystal structure determination was performed on a *Bruker D8 VENTURE KAPPA* diffractometer with a microfocus sealed tube using a multilayer mirror as the monochromator and a *Bruker PHOTON III* detector. As characteristic X-ray radiation MoK_α (λ = 71.073 pm) was used for the measurements. Before the measurements, the crystals were prepared in perfluorinated ether oil (Fomblin® YR-180) and selected using a light microscope with equipped polarization filter. A suitable single crystal was fixed on a MiTeGen micromount (150 µm polymer loop) and adjusted to the X-ray beam and cooled down to 100 K in a stream of N_2. The images with the intensity data were processed using the software *APEX5*.[6] The frames were integrated with the Bruker *SAINT* software package using a narrow frame algorithm. Absorption effects were corrected using SADABS for the multi-scan absorption correction.[7-8] The structure solution and refinement were done with the software *OLEX2*.[9] Dual methods using *SHELXT* were used for structure solution and full-matrix least-squares methods against F^2 using *SHELXL* for the refinement.[10-11] All illustrations of the crystal structures were made with the program *Diamond 4* using the .cif as the input file.[12]

Powder X-Ray Diffraction and Rietveld Refinement

P-XRD data was collected on a *Stoe* Stadi-P powder diffractometer with a *Mythen* detector and a Debye−Scherrer geometry by using Mo-$K_{\alpha1}$ radiation of λ = 0.70930 Å. The samples were ground and sealed in glass capillaries with 0.5 mm or 0.3 mm diameter. The data was recorded in a range of 2θ = 0 - 60° within 10.5 h. The Rietveld refinement was performed using the software *TOPAS-Academic (64 V6)*.[13-14] The refinement process included the scale factor, lattice parameters, atomic positions and the isotropic atomic displacement parameters for a.) all atoms except hydrogen (compound **1**) and b.) only the selenium atoms (mixture of compound **1** and compound **2**), along with corrections for zero shift, specimen displacement, and background. Peak profiles were described using the pseudo-Voigt function of Thompson, Cox, and Hastings,[15] with the profile shape parameters u, v, w, and y refined accordingly.

$[Se_4][HS_2O_7]_2$ (1)

Table S1: Crystallographic data of $[Se_4][HS_2O_7]_2$.

Empirical formula	$H_2O_{14}S_4Se_4$
Formula weight	670.10 g/mol
Temperature	100.00 K
Crystal system	monoclinic
Space group	$P2_1/n$ (No. 14)
Unit cell dimensions	a = 768.7(1) pm b = 555.53(8) pm c = 1620.1(3) pm β = 96.965(5)°
Volume	686.8(2) Å^3
Z	2
ρ_{calc}	3.241 g/cm^3
μ	11.365 mm^{-1}
F(000)	628
Crystal size	0.39 × 0.09 × 0.08 mm^3
Radiation	MoK$_\alpha$ (λ = 0.71073 nm)
2Θ range for data collection	5.626 to 60.994
Index ranges	-10 ≤ h ≤ 10, -7 ≤ k ≤ 7, -23 ≤ l ≤ 23
Reflections collected	22721
Independent reflections	2079 [R_{int} = 0.0591, R_σ = 0.0359]
Completeness	99.5%
Absorption correction	multiscan
Min. and max. transmission	0.281 / 0.746
Data/restraints/parameters	2079/0/105
Goodness-of-fit on F^2	1.086
Final R indexes [I≥2σ (I)]	R_1 = 0.0264, wR_2 = 0.0657
Final R indexes [all data]	R_1 = 0.0269, wR_2 = 0.0661
Largest diff. peak/hole	1.00/–0.82 e · Å^{-3}
CCDC-No.	2477856

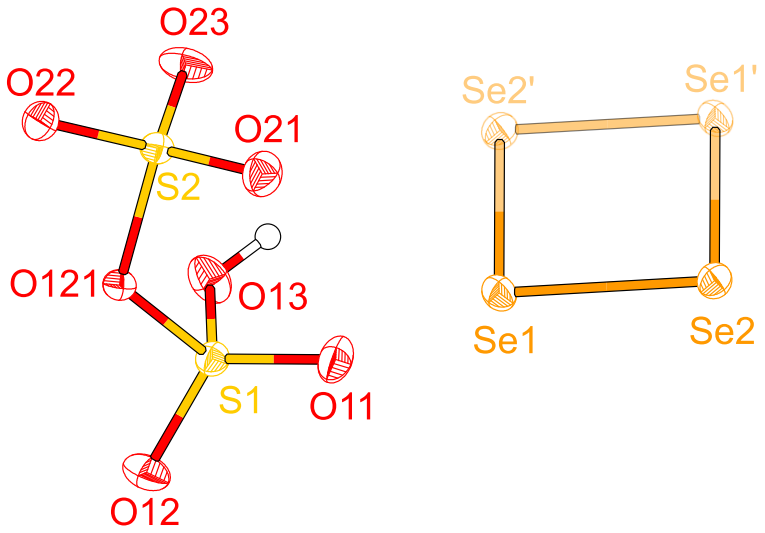

Figure S1: Thermal ellipsoid plot of the asymmetric unit of $[Se_4][HS_2O_7]_2$ shown with 50% probability. Atoms that are generated by symmetry operation for complete representation of the cation are shown at 50% visibility.

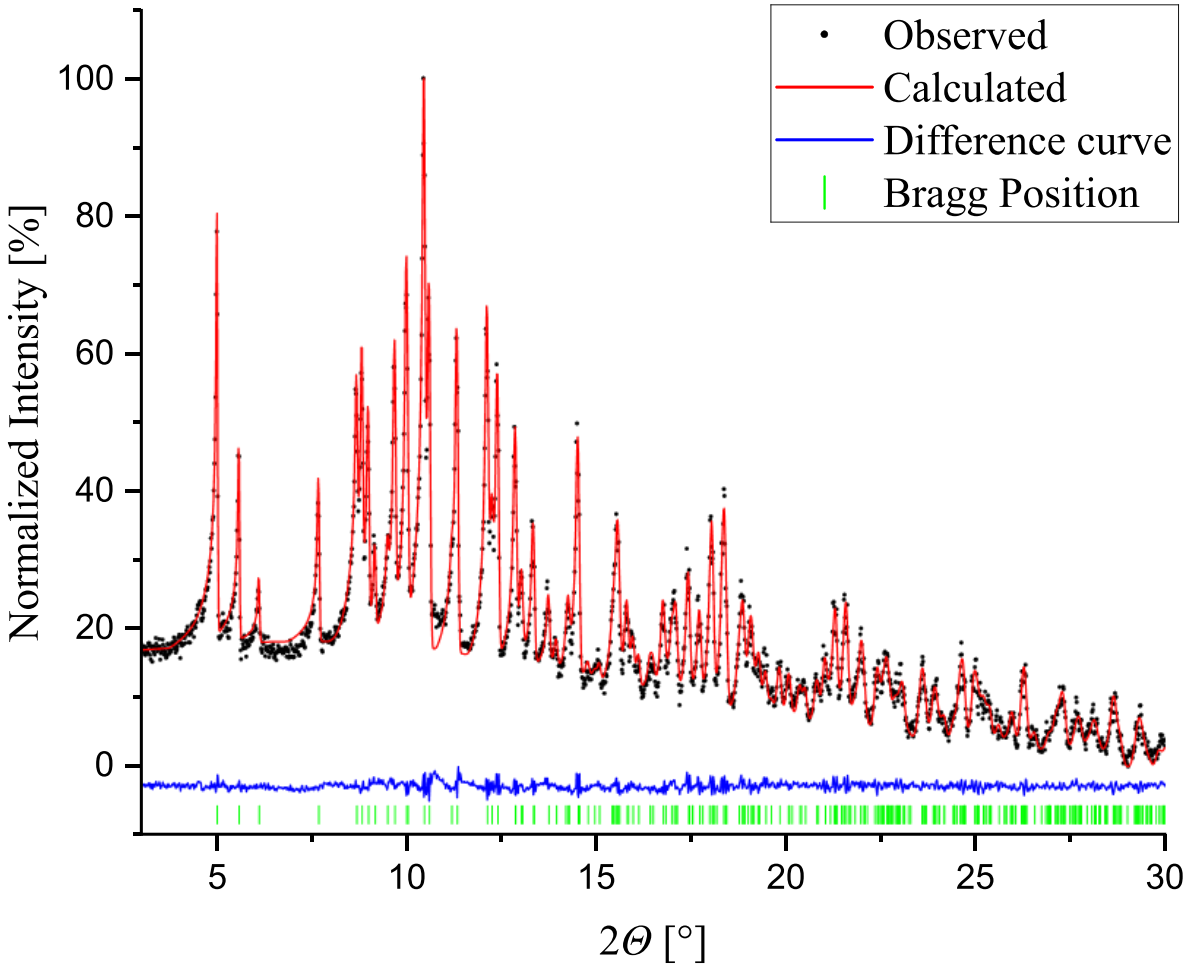

Figure S 2: Powder X-Ray Diffraction Pattern from the prepared $[Se_4][HS_2O_7]_2$ (black) versus the calculated curve (red). The difference curve is shown below in blue. Experimental and calculated data were normalized to [0, 100] and the difference data to [-5, 0], respectively.

Table S2: Fractional Atomic Coordinates ($\times 10^4$) and Equivalent Isotropic Displacement Parameters ($Å^2 \times 10^3$) for $[Se_4][HS_2O_7]_2$. U_{eq} is defined as 1/3 of the trace of the orthogonalised U_{IJ} tensor.

Atom	*x*	*y*	*z*	U(eq)
Se1	10124.7(3)	7737.8(4)	4382.2(2)	10.30(9)
Se2	7894.1(3)	9703.0(4)	4909.1(2)	10.25(9)
S1	5392.7(6)	8400.9(9)	2447.4(3)	8.99(11)
S2	4861.8(7)	5402.4(8)	3829.6(3)	8.95(12)
O11	6952(2)	9242(3)	2923.8(10)	13.8(3)
O12	5319(2)	7941(3)	1584.6(10)	13.6(3)
O13	3842(2)	10048(3)	2566.2(11)	14.5(3)
O21	6663(2)	5604(3)	4193.1(10)	14.0(3)
O22	4190(2)	2971(3)	3814.9(10)	14.1(3)
O23	3716(2)	7213(3)	4100.4(11)	15.5(3)
O121	4857(2)	5881(3)	2817.9(9)	9.8(3)

Table S3: Anisotropic Displacement Parameters ($Å^2 \times 10^3$) for $[Se_4][HS_2O_7]_2$. The anisotropic displacement factor exponent takes the form: $-2\pi^2[h^2a^{*2}U_{11}+2hka^*b^*U_{12}+\ldots]$.

Atom	U_{11}	U_{22}	U_{33}	U_{23}	U_{13}	U_{12}
Se1	10.68(13)	9.75(12)	10.63(13)	-2.84(6)	1.97(8)	-0.13(6)
Se2	7.49(12)	12.05(12)	11.31(13)	-1.63(6)	1.51(8)	-0.40(6)
S1	8.7(2)	9.3(2)	8.9(2)	0.50(16)	0.77(16)	-0.38(16)
S2	9.6(2)	9.1(2)	8.5(2)	-0.87(15)	2.46(17)	-0.63(16)
O11	10.9(7)	14.6(7)	15.2(7)	1.9(6)	-1.2(6)	-4.2(6)
O12	18.6(8)	14.0(7)	8.4(7)	0.4(5)	2.5(6)	2.1(6)
O13	13.8(8)	14.0(7)	15.0(8)	-4.1(6)	-1.0(6)	4.0(6)
O21	12.1(7)	15.6(7)	13.5(7)	1.2(5)	-1.0(6)	-1.8(5)
O22	19.7(8)	10.6(6)	12.6(7)	-0.7(5)	4.6(6)	-6.2(6)
O23	19.4(8)	15.6(7)	12.8(7)	-2.1(6)	7.2(6)	4.8(6)
O121	11.8(7)	10.4(6)	7.7(6)	-1.0(5)	2.8(5)	-2.7(5)

Table S4: Bond Lengths for $[Se_4][HS_2O_7]_2$ in pm.

Atom	Atom	Length/pm	Atom	Atom	Length/pm
Se1	Se2	228.37(4)	S1	O121	159.70(15)
Se1	Se2[1]	228.80(3)	S2	O21	144.15(17)
S1	O11	142.36(16)	S2	O22	144.52(15)
S1	O12	141.53(17)	S2	O23	144.02(16)
S1	O13	153.30(17)	S2	O121	166.00(16)

[1]2-X, 2-Y, 1-Z

Table S5: Bond Angles for $[Se_4][HS_2O_7]_2$.

Atom	Atom	Atom	Angle/°	Atom	Atom	Atom	Angle/°
Se2	Se1	Se2[1]	89.980(14)	O21	S2	O22	113.78(10)
Se1	Se2	Se1[1]	90.021(14)	O21	S2	O121	106.13(9)
O11	S1	O13	110.64(10)	O22	S2	O121	100.09(9)
O11	S1	O121	108.81(9)	O23	S2	O21	114.44(10)
O12	S1	O11	121.68(11)	O23	S2	O22	115.29(10)
O12	S1	O13	107.03(10)	O23	S2	O121	105.11(9)
O12	S1	O121	103.39(9)	S1	O121	S2	122.80(9)
O13	S1	O121	103.66(9)				

[1]2-X, 2-Y, 1-Z

Table S6: Torsion Angles for $[Se_4][HS_2O_7]_2$.

A	B	C	D	Angle/°	A	B	C	D	Angle/°
O11	S1	O121	S2	45.43(14)	O21	S2	O121	S1	-64.80(13)
O12	S1	O121	S2	176.08(11)	O22	S2	O121	S1	176.67(11)
O13	S1	O121	S2	-72.35(13)	O23	S2	O121	S1	56.83(14)

Table S7: Hydrogen Atom Coordinates ($Å \times 10^4$) and Isotropic Displacement Parameters ($Å^2 \times 10^3$) for $[Se_4][HS_2O_7]_2$.

Atom	*x*	*y*	*z*	U(eq)
H13	4080(50)	10800(7)	2960(30)	30(10)

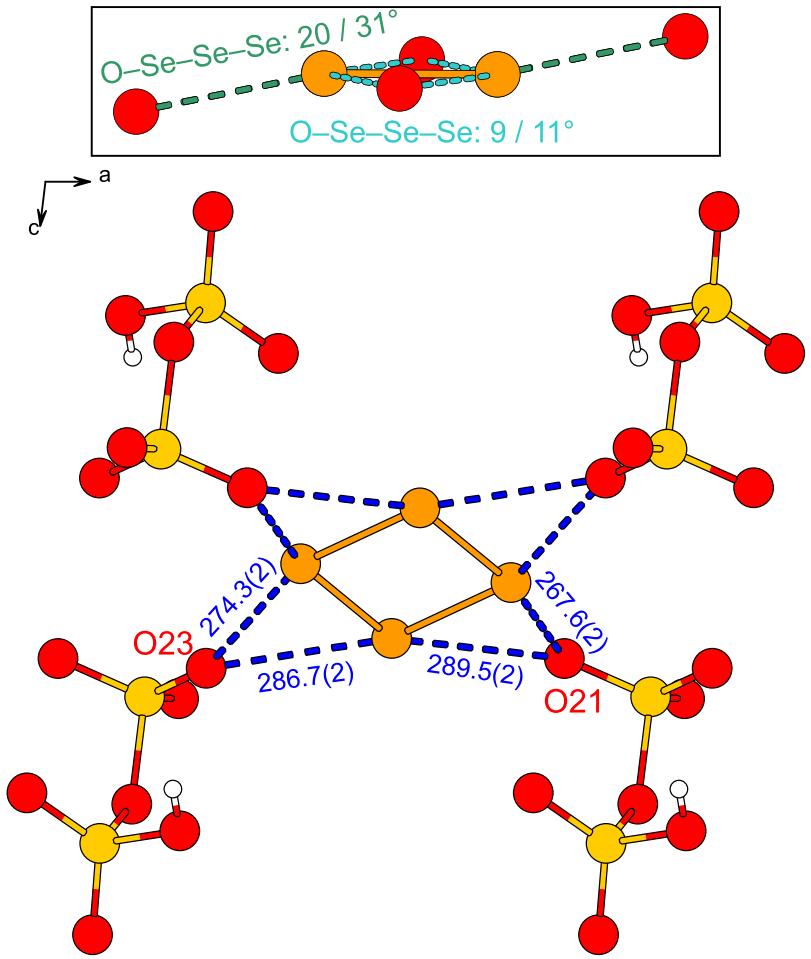

Figure S 3: Chalcogen-bonding (D–A distance below 300 pm) within $[Se_4][HS_2O_7]_2$. Distances are given in pm. O–Se coordination within the $[Se_4]$ plane and O–Se–Se–Se torsion angles are shown at the top.

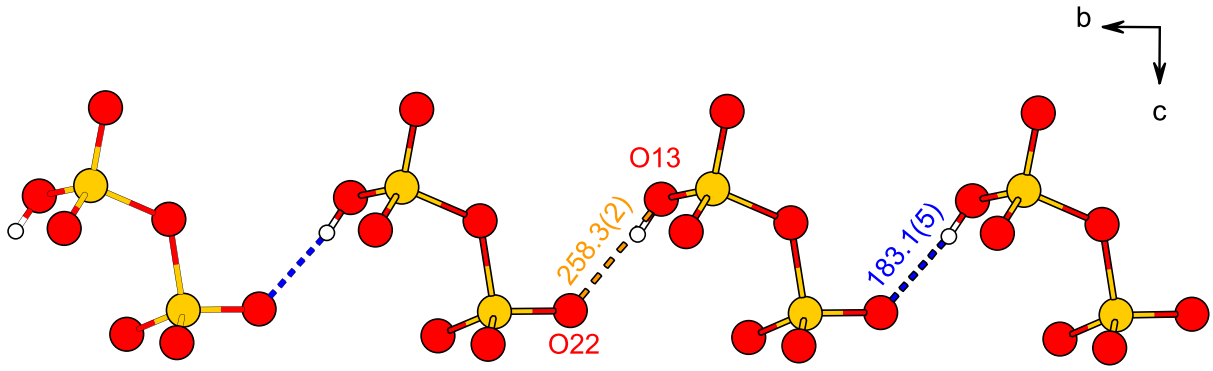

Figure S 4: Hydrogen-bonding within $[Se_4][HS_2O_7]_2$. Distances are given in pm.

$[Se_4][S_2O_7]$ (2)

Table S8: Crystallographic data of $[Se_4][S_2O_7]$.

Empirical formula	$O_7S_2Se_4$
Formula weight	491.96 g/mol
Temperature	100.00 K
Crystal system	monoclinic
Space group	$P2_1/c$ (No. 14)
Unit cell dimensions	a = 557.77(4) pm b = 2237.38(16) pm c = 711.12(5) pm β = 100.154(2)°
Volume	873.54(11) Å^3
Z	4
ρ_{calc}	3.741 g/cm^3
μ	17.278 mm^{-1}
F(000)	869
Crystal size	0.5 × 0.2 × 0.15 mm^3
Radiation	MoK$_\alpha$ (λ = 0.71073 nm)
2Θ range for data collection	6.098 to 61.04
Index ranges	-6 ≤ h ≤ 7, -31 ≤ k ≤ 31, -10 ≤ l ≤ 10
Reflections collected	35113
Independent reflections	2599 [R_{int} = 0.0552, R_σ = 0.0302]
Completeness	98.1%
Absorption correction	multiscan
Min. and max. transmission	0.357 / 0.746
Data/restraints/parameters	2599/0/119
Goodness-of-fit on F^2	1.142
Final R indexes [I≥2σ (I)]	R_1 = 0.0221, wR_2 = 0.0455
Final R indexes [all data]	R_1 = 0.0241, wR_2 = 0.0471
Largest diff. peak/hole	1.00/–0.98 e · Å^{-3}
CCDC-No.	2504489

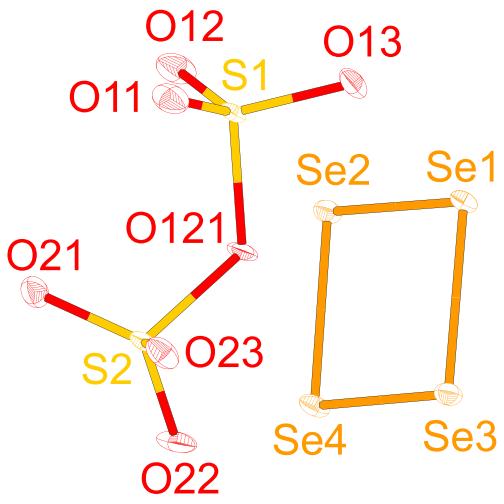

Figure S5: Thermal ellipsoid plot of the asymmetric unit of $[Se_4][S_2O_7]$ shown with 50% probability. Atoms that are generated by symmetry operation for complete representation of the cation are shown at 50% visibility.

Table S9: Fractional Atomic Coordinates ($\times 10^4$) and Equivalent Isotropic Displacement Parameters ($Å^2 \times 10^3$) for $[Se_4][S_2O_7]$. U_{eq} is defined as 1/3 of the trace of the orthogonalised U_{IJ} tensor.

Atom	*x*	*y*	*z*	U(eq)
Se1	4411.2(4)	3057.2(2)	-1543.1(3)	9.20(6)
Se2	6819.5(4)	3465.8(2)	-3497.4(3)	10.09(6)
Se3	2852.8(4)	3979.7(2)	-1114.2(3)	10.15(6)
Se4	5201.9(4)	4388.8(2)	-3105.1(3)	10.84(6)
S1	9729.9(9)	3143.9(2)	2407.2(7)	8.51(10)
S2	9213.7(9)	4412.1(2)	2865.1(7)	9.07(10)
O11	11092(3)	3199.8(7)	4306(2)	16.7(3)
O12	11184(3)	3101.4(7)	922(3)	19.6(4)
O13	7743(3)	2719.9(7)	2191(2)	14.3(3)
O21	11731(3)	4448.7(7)	2675(2)	14.2(3)
O22	7583(3)	4814.2(7)	1660(2)	16.5(3)
O23	8803(3)	4388.1(7)	4826(2)	13.8(3)
O121	8193(3)	3770.6(6)	1931(2)	12.3(3)

Table S10: Anisotropic Displacement Parameters ($Å^2 \times 10^3$) for $[Se_4][S_2O_7]$. The anisotropic displacement factor exponent takes the form: $-2\pi^2[h^2a^{*2}U_{11}+2hka^*b^*U_{12}+\ldots]$.

Atom	U_{11}	U_{22}	U_{33}	U_{23}	U_{13}	U_{12}
Se1	12.15(10)	5.23(10)	10.29(11)	0.71(7)	2.19(7)	-0.23(7)
Se2	12.2(1)	7.28(10)	11.59(11)	-0.73(7)	4.23(7)	0.32(7)
Se3	11.62(10)	7.16(10)	12.32(11)	-0.64(7)	3.90(7)	0.97(7)
Se4	14.93(10)	5.54(10)	12.55(11)	1.67(7)	3.81(8)	0.22(7)
S1	11.6(2)	3.8(2)	10.4(2)	0.05(16)	2.62(17)	-0.26(16)
S2	12.8(2)	4.1(2)	10.8(2)	-1.12(16)	3.20(17)	-0.10(16)
O11	20.8(8)	11.0(7)	15.5(8)	2.2(6)	-4.6(6)	1.1(6)
O12	25.9(9)	11.5(8)	26.0(10)	-1.0(6)	17.5(7)	0.3(6)
O13	15.9(7)	7.8(7)	18.8(8)	0.6(6)	2.1(6)	-4.0(6)
O21	14.1(7)	11.7(7)	18.6(8)	-2.9(6)	7.8(6)	-2.9(6)
O22	22.9(8)	6.9(7)	18.7(8)	0.6(6)	0.5(6)	4.9(6)
O23	20.2(8)	10.3(7)	12.5(8)	-2.5(6)	7.3(6)	-3.2(6)
O121	14.7(7)	3.9(7)	16.5(8)	-2.1(5)	-2.3(6)	1.6(5)

Table S11: Bond Lengths for $[Se_4][S_2O_7]$ in pm.

Atom	Atom	Length/pm	Atom	Atom	Length/pm
Se1	Se2	228.69(3)	S1	O13	144.62(16)
Se1	Se3	228.09(3)	S1	O121	164.69(15)
Se2	Se4	229.04(3)	S2	O21	143.65(16)
Se3	Se4	228.32(3)	S2	O22	144.75(16)
S1	O11	143.31(17)	S2	O23	145.36(17)
S1	O12	144.38(18)	S2	O121	164.08(15)

Table S12: Bond Angles for $[Se_4][S_2O_7]$.

Atom	Atom	Atom	Angle/°	Atom	Atom	Atom	Angle/°
Se3	Se1	Se2	89.886(11)	O13	S1	O121	100.10(9)
Se1	Se2	Se4	90.013(11)	O21	S2	O22	115.56(10)
Se1	Se3	Se4	90.344(11)	O21	S2	O23	114.47(10)
Se3	Se4	Se2	89.741(10)	O21	S2	O121	106.67(9)
O11	S1	O12	114.97(11)	O22	S2	O23	113.71(10)
O11	S1	O13	115.24(10)	O22	S2	O121	99.63(9)
O11	S1	O121	106.83(9)	O23	S2	O121	104.71(9)
O12	S1	O13	113.43(10)	S2	O121	S1	122.06(10)
O12	S1	O121	104.17(9)				

Table S13: Torsion Angles for $[Se_4][S_2O_7]$.

A	B	C	D	Angle/°	A	B	C	D	Angle/°
O11	S1	O121	S2	30.39(15)	O21	S2	O121	S1	45.76(15)
O12	S1	O121	S2	-91.69(14)	O22	S2	O121	S1	166.27(13)
O13	S1	O121	S2	150.82(12)	O23	S2	O121	S1	-75.94(14)

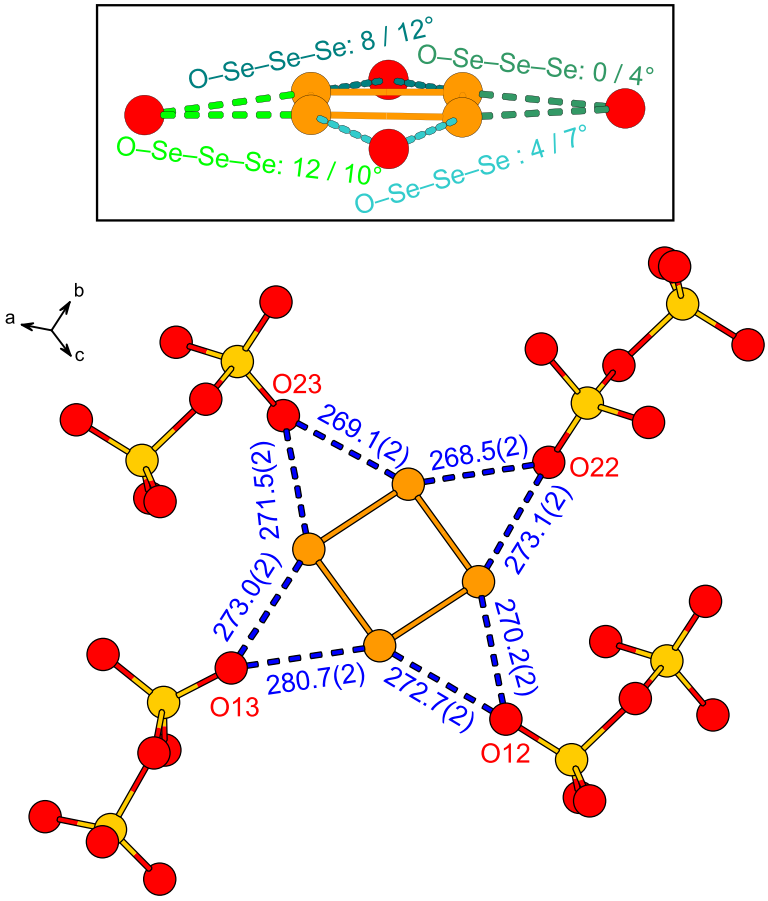

Figure S 6: Chalcogen-bonding (D–A distance below 300 pm) within $[Se_4][S_2O_7]$. Distances are given in pm. O–Se coordination within the $[Se_4]$ plane and O–Se–Se–Se torsion angles are shown at the top.

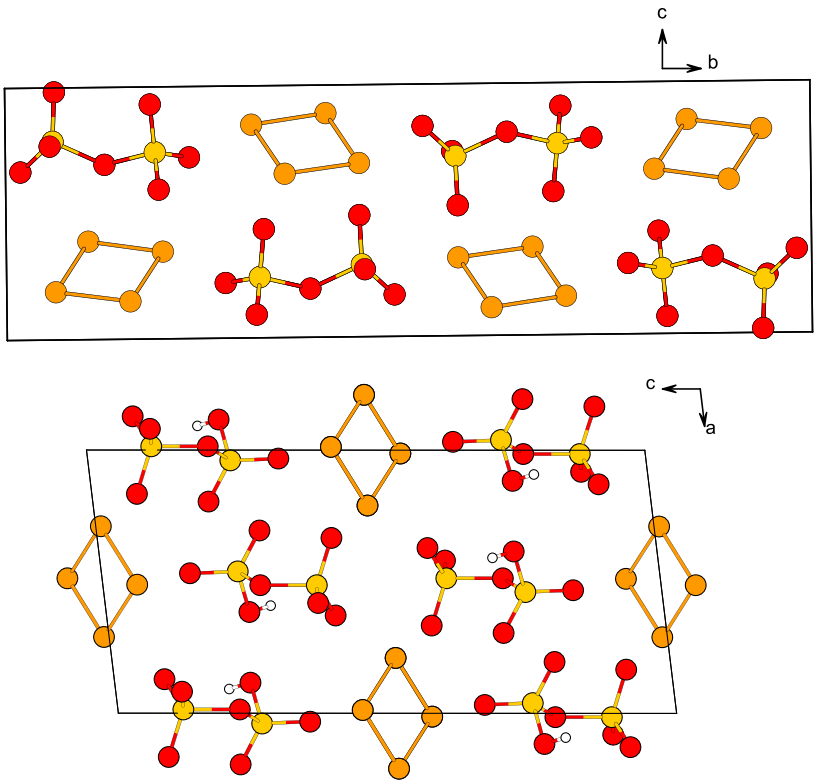

Figure S 7: Packed unit cells of [Se4][S2O7] (top) and [Se4][HS2O7]2 (bottom) viewed along the crystallographic a- and b-axis, respectively.

$[Se_4][HS_3O_{10}]_2$ (3)

Table S14: Crystallographic data of $[Se_4][HS_3O_{10}]_2$.

Empirical formula	$H_2O_{20}S_6Se_4$
Formula weight	830.22 g/mol
Temperature	100.00 K
Crystal system	monoclinic
Space group	$P2_1/n$ (No. 14)
Unit cell dimensions	a = 967.36(7) pm b = 983.62(6) pm c = 1987.30(7) pm β = 95.883(3)°
Volume	934.48(11) Å^3
Z	2
ρ_{calc}	2.951 g/cm^3
μ	8.622 mm^{-1}
F(000)	788
Crystal size	0.06 × 0.03 × 0.03 mm^3
Radiation	MoK$_\alpha$ (λ = 0.71073 nm)
2Θ range for data collection	5.616 to 57.382
Index ranges	-13 ≤ h ≤ 12, -13 ≤ k ≤ 13, -13 ≤ l ≤ 13
Reflections collected	15582
Independent reflections	2411 [R_{int} = 0.0581, R_σ = 0.0415]
Completeness	100%
Absorption correction	multiscan
Min. and max. transmission	0.595 / 0.746
Data/restraints/parameters	2411/0/137
Goodness-of-fit on F^2	1.057
Final R indexes [I≥2σ (I)]	R_1 = 0.0378, wR_2 = 0.0847
Final R indexes [all data]	R_1 = 0.0521, wR_2 = 0.0908
Largest diff. peak/hole	1.00/–0.72 e · Å^{-3}
CCDC-No.	2476927

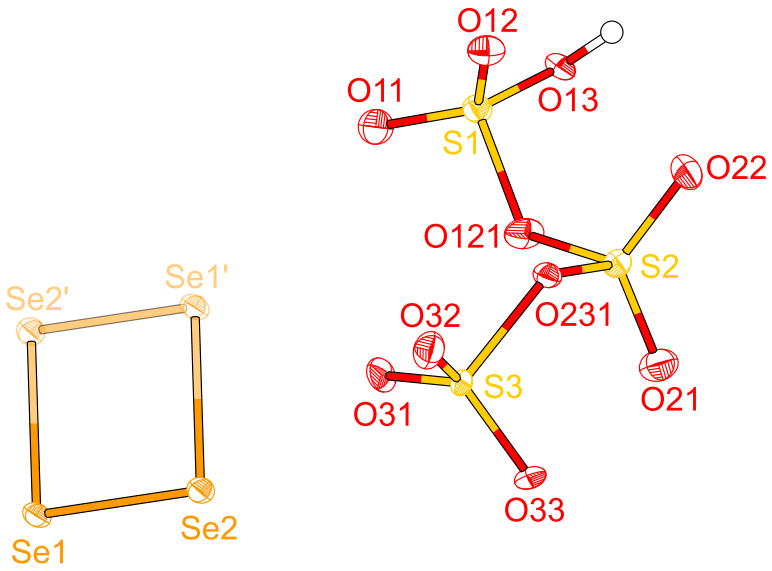

Figure S8: Thermal ellipsoid plot of the asymmetric unit of $[Se_4][HS_3O_{10}]_2$ shown with 50% probability. Atoms that are generated by symmetry operation for complete representation of the cation are shown at 50% visibility.

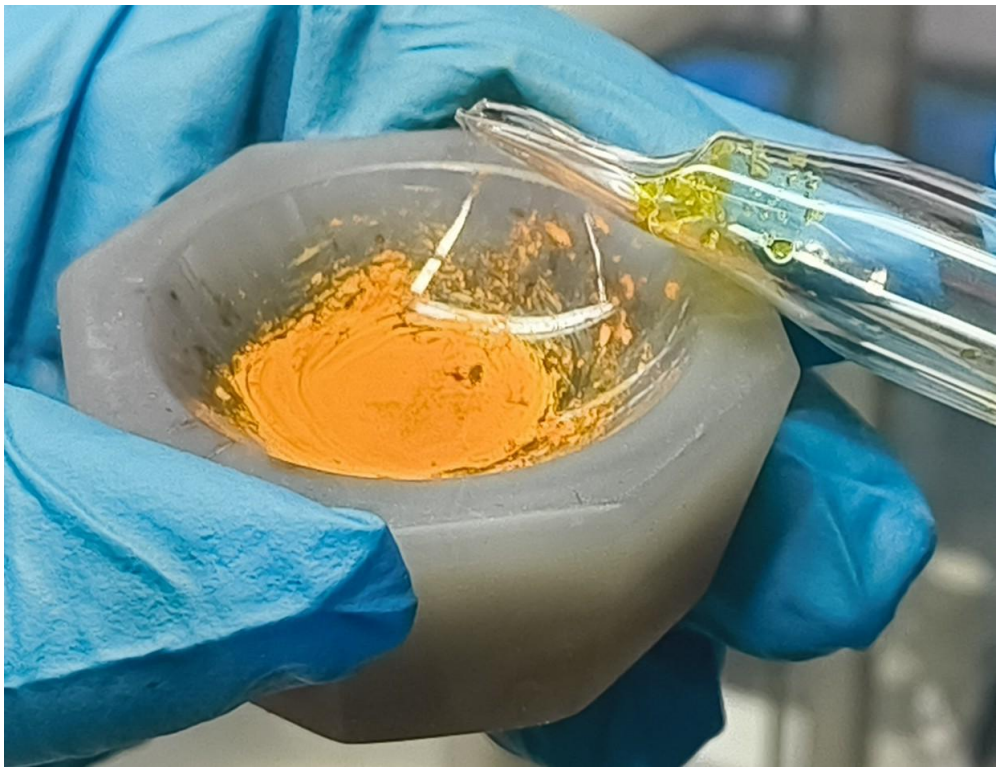

Figure S 9: Single crystals of $[Se_4][HS_3O_{10}]_2$ in a freshly cracked glass ampoule (right) and powdered sample in a mortar (left).

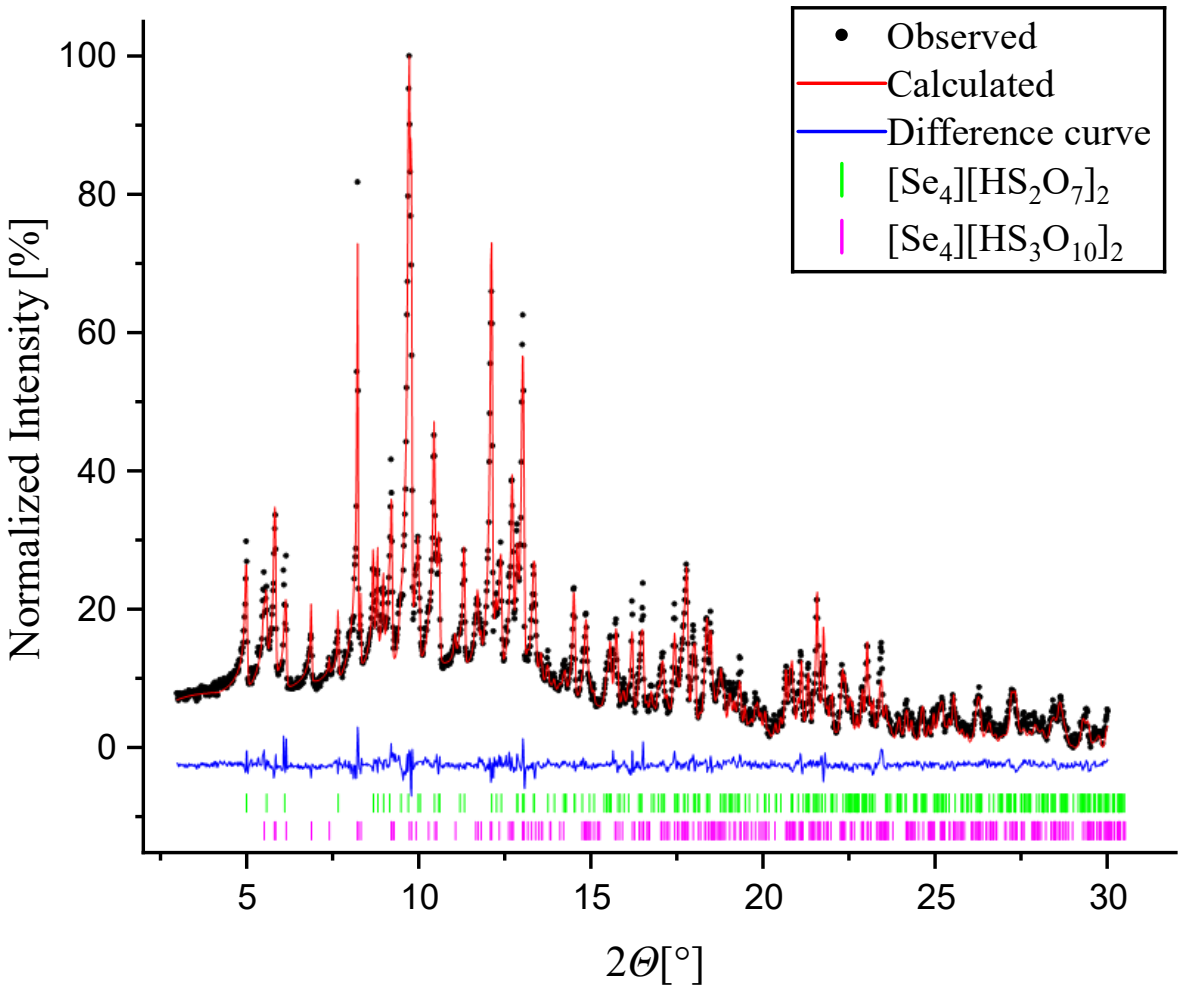

Figure S 10: Powder X-Ray Diffraction Pattern from the prepared $[Se_4][HS_3O_{10}]_2$ (black) versus the calculated curve (red). The difference curve is shown below in blue. Experimental and calculated data were normalized to [0, 100] and the difference data to [-7, 3], respectively. The Bragg positions for $[Se_4][HS_2O_7]_2$ and $[Se_4][HS_3O_{10}]_2$ from single crystal data are shown as green and magenta bars, respectively.

Table S15: Fractional Atomic Coordinates ($\times 10^4$) and Equivalent Isotropic Displacement Parameters ($Å^2 \times 10^3$) for $[Se_4][HS_3O_{10}]_2$. U_{eq} is defined as 1/3 of the trace of the orthogonalised U_{IJ} tensor.

Atom	*x*	*y*	*z*	U(eq)
Se1	5354.0(5)	8908.8(4)	3856.3(4)	12.79(13)
Se2	3874.7(5)	10714.2(4)	3906.6(4)	13.12(13)
S1	5142.0(12)	5006.7(11)	1984.7(11)	13.2(2)
S2	7060.5(12)	3877.5(11)	4078.0(11)	13.8(2)
S3	8461.1(12)	6290.2(10)	5176.5(11)	12.6(2)
O11	4269(4)	6142(3)	2046(3)	21.1(8)
O12	6304(3)	5021(3)	1229(3)	17.3(7)
O13	4192(4)	3716(3)	1674(3)	21.8(8)
O21	6876(4)	3491(4)	5424(3)	20.9(7)
O22	7306(4)	2909(3)	3077(3)	22.2(8)
O31	7190(3)	7042(3)	4980(3)	18.3(7)
O32	9651(4)	6877(3)	4654(3)	19.6(7)
O33	8733(4)	5639(3)	6471(3)	16.3(7)
O121	5674(3)	4728(3)	3588(3)	18.0(7)
O231	8196(3)	4989(3)	4031(3)	12.2(6)

Table S16: Anisotropic Displacement Parameters ($Å^2 \times 10^3$) for $[Se_4][HS_3O_{10}]_2$. The anisotropic displacement factor exponent takes the form: $-2\pi^2[h^2a^{*2}U_{11}+2hka^*b^*U_{12}+\ldots]$.

Atom	U_{11}	U_{22}	U_{33}	U_{23}	U_{13}	U_{12}
Se1	14.1(2)	13.1(2)	10.6(2)	-3.62(16)	-1.14(17)	3.80(17)
Se2	14.0(2)	13.5(2)	11.0(2)	-1.87(16)	-3.08(16)	4.59(17)
S1	13.1(5)	13.5(5)	12.5(5)	-1.3(4)	-0.7(4)	1.4(4)
S2	15.6(6)	13.0(5)	12.4(5)	0.7(4)	-1.4(4)	1.6(4)
S3	17.0(6)	9.3(5)	10.6(5)	0.4(4)	-3.0(4)	4.8(4)
O11	21.5(19)	22.1(17)	19.2(17)	-0.7(14)	-0.2(14)	7.6(14)
O12	16.4(17)	21.6(17)	14.0(16)	-1.0(13)	2.3(13)	-0.1(14)
O13	37(2)	15.2(16)	12.4(16)	-5.2(13)	-0.7(15)	8.0(15)
O21	24.0(19)	22.8(17)	15.5(16)	1.5(14)	-0.6(14)	-3.6(15)
O22	30(2)	14.6(15)	20.6(18)	-4.3(14)	-2.4(15)	3.0(15)
O31	17.7(18)	15.9(15)	19.9(17)	-4.4(13)	-5.0(14)	9.2(14)
O32	21.4(18)	15.4(16)	21.3(17)	3.0(13)	-1.1(14)	-1.1(14)
O33	22.9(18)	17.4(16)	7.6(14)	0.9(12)	-3.2(13)	3.4(14)
O121	11.2(16)	27.5(18)	14.5(16)	-1.4(14)	-2.7(13)	5.6(14)
O231	13.4(16)	13.1(14)	10.2(14)	-1.6(11)	1.4(12)	1.7(12)

Table S17: Bond Lengths for $[Se_4][HS_3O_{10}]_2$ in pm.

Atom	Atom	Length/pm	Atom	Atom	Length/pm
Se1	Se2	228.44(6)	S2	O22	141.0(3)
Se1	Se2[1]	228.80(6)	S2	O121	161.3(3)
S1	O11	140.5(3)	S2	O231	155.4(3)
S1	O12	141.2(3)	S3	O31	143.1(3)
S1	O13	157.9(4)	S3	O32	143.0(4)
S1	O121	163.6(3)	S3	O33	143.0(3)
S2	O21	141.1(3)	S3	O231	171.0(3)

[1]1-X, 2-Y, 1-Z

Table S18: Bond Angles for $[Se_4][HS_3O_{10}]_2$.

Atom	Atom	Atom	Angle/°	Atom	Atom	Atom	Angle/°
Se2	Se1	Se2[1]	89.77(2)	O22	S2	O121	109.5(2)
Se1	Se2	Se1[1]	90.23(2)	O22	S2	O231	106.5(2)
O11	S1	O12	122.0(2)	O231	S2	O121	101.22(18)
O11	S1	O13	107.9(2)	O31	S3	O231	103.21(17)
O11	S1	O121	102.85(19)	O32	S3	O31	117.1(2)
O12	S1	O13	112.60(19)	O32	S3	O33	115.0(2)
O12	S1	O121	108.94(18)	O32	S3	O231	97.76(18)
O13	S1	O121	99.92(18)	O33	S3	O31	115.4(2)
O21	S2	O121	103.9(2)	O33	S3	O231	104.94(17)
O21	S2	O231	112.07(19)	S2	O121	S1	123.1(2)
O22	S2	O21	121.7(2)	S2	O231	S3	124.42(19)

[1]1-X, 2-Y, 1-Z

Table S19: Torsion Angles for$[Se_4][HS_3O_{10}]_2$.

A	B	C	D	Angle/°	A	B	C	D	Angle/°
O11	S1	O121	S2	-159.1(3)	O22	S2	O231	S3	-172.5(2)
O12	S1	O121	S2	-28.4(3)	O31	S3	O231	S2	-63.2(3)
O13	S1	O121	S2	89.8(3)	O32	S3	O231	S2	176.5(2)
O21	S2	O121	S1	-160.7(3)	O33	S3	O231	S2	58.0(3)
O21	S2	O231	S3	-37.1(3)	O121	S2	O231	S3	73.0(2)
O22	S2	O121	S1	-29.2(3)	O231	S2	O121	S1	83.0(3)

Table S20: Hydrogen Atom Coordinates ($Å \times 10^4$) and Isotropic Displacement Parameters ($Å^2 \times 10^3$) for $[Se_4][HS_3O_{10}]_2$.

Atom	*x*	*y*	*z*	U(eq)
H13	4650.97	3104.28	1329.64	33

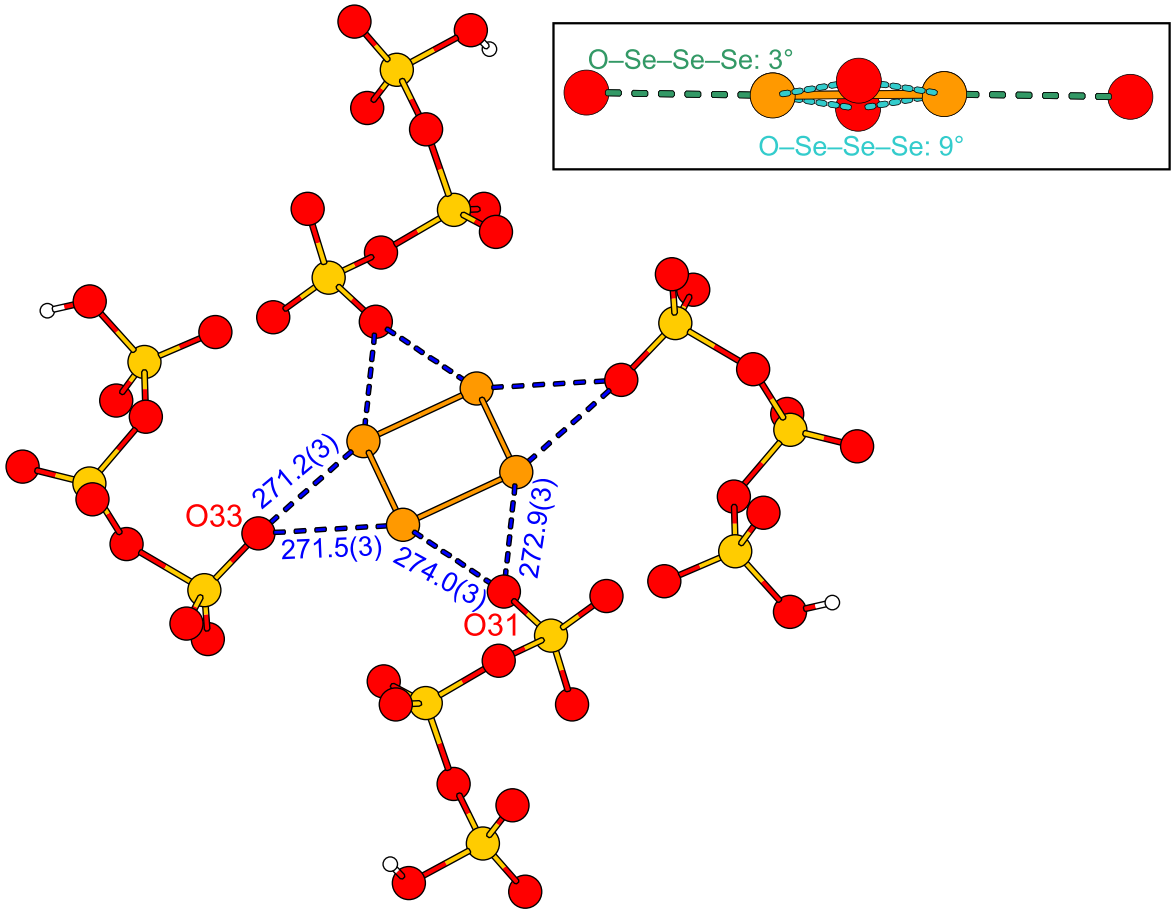

Figure S 11: Chalcogen-bonding (D–A distance below 300 pm) within $[Se_4][HS_3O_{10}]_2$. Distances are given in pm. O–Se coordination within the $[Se_4]$ plane and O–Se–Se–Se torsion angles are shown in the top right corner.

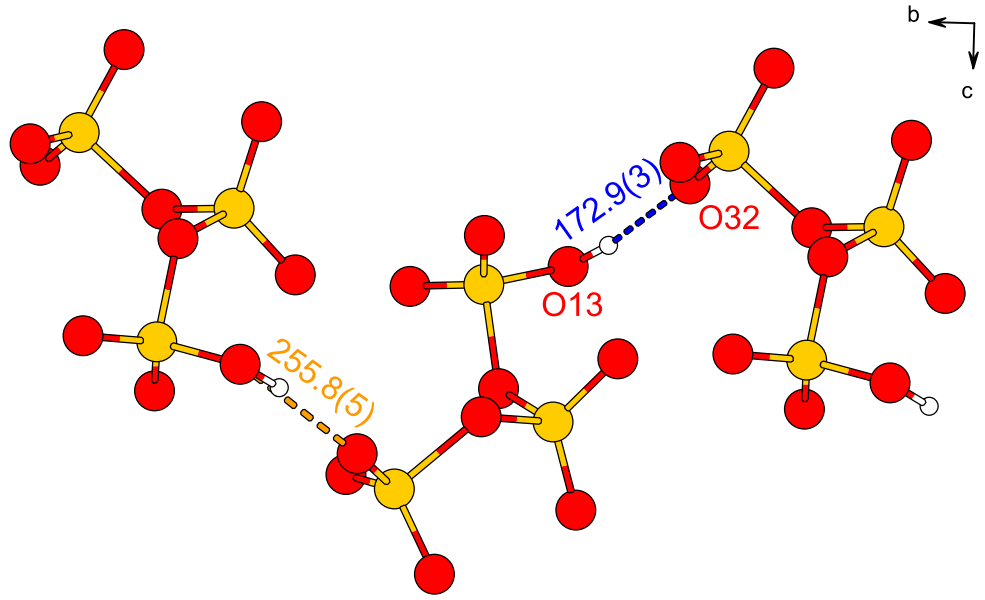

Figure S 12: Hydrogen-bonding within $[Se_4][HS_3O_{10}]_2$. Distances are given in pm.

$[Te_4][HS_3O_{10}]_2$ (4)

Table S21: Crystallographic data of $[Te_4][HS_3O_{10}]_2$.

Empirical formula	$H_2O_{20}S_6Te_4$
Formula weight	1024.78 g/mol
Temperature	100.00 K
Crystal system	monoclinic
Space group	$P2_1/n$ (No. 14)
Unit cell dimensions	a = 1003.36(3) pm b = 1014.61(2) pm c = 1044.79(3) pm β = 96.4010(10)°
Volume	1056.99(5) Å^3
Z	2
ρ_{calc}	3.220 g/cm^3
μ	6.146 mm^{-1}
F(000)	932
Crystal size	0.11 × 0.03 × 0.01 mm^3
Radiation	MoK$_\alpha$ (λ = 0.71073 nm)
2Θ range for data collection	5.34 to 59.142
Index ranges	-13 ≤ h ≤ 12, -14 ≤ k ≤ 11, -14 ≤ l ≤ 14
Reflections collected	10436
Independent reflections	2951 [R_{int} = 0.0415, R_σ = 0.0388]
Completeness	99.9%
Absorption correction	Multiscan
Min. and max. transmission	0.633 / 0.747
Data/restraints/parameters	2951/0/137
Goodness-of-fit on F^2	1.069
Final R indexes [I≥2σ (I)]	R_1 = 0.0313, wR_2 = 0.0643
Final R indexes [all data]	R_1 = 0.0400, wR_2 = 0.0681
Largest diff. peak/hole	1.22/–0.91 e · Å^{-3}
CCDC-No.	2476926

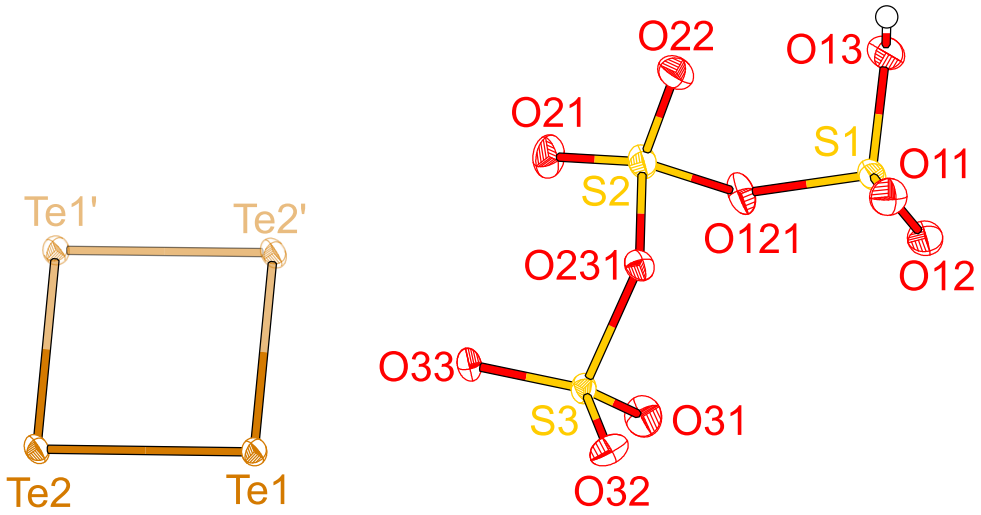

Figure S13: Thermal ellipsoid plot of the asymmetric unit of $[Te_4][HS_3O_{10}]_2$ shown with 50% probability. Atoms that are generated by symmetry operation for complete representation of the cation are shown at 50% visibility.

Table S22: Fractional Atomic Coordinates ($\times 10^4$) and Equivalent Isotropic Displacement Parameters ($Å^2 \times 10^3$) for $[Te_4][HS_3O_{10}]_2$. U_{eq} is defined as 1/3 of the trace of the orthogonalised U_{IJ} tensor.

Atom	*x*	*y*	*z*	U(eq)
Te1	1283.3(3)	6194.3(3)	-483.2(3)	13.42(8)
Te2	1277.7(3)	4323.1(3)	1308.6(3)	14.08(8)
S1	8024.1(11)	5054.1(10)	4689.5(11)	14.5(2)
S2	5794.8(11)	4099.4(11)	2999.5(11)	15.9(2)
S3	5057.0(11)	6348.4(10)	1393.8(11)	12.9(2)
O11	8754(3)	4975(3)	3607(3)	20.5(7)
O12	8113(3)	6179(3)	5494(3)	20.0(7)
O13	8207(4)	3816(3)	5510(3)	19.7(7)
O21	4426(3)	4002(3)	3163(3)	22.2(7)
O22	6610(3)	2978(3)	2910(3)	23.1(8)
O31	5184(4)	7141(3)	2527(3)	22.0(7)
O32	5757(3)	6787(3)	346(3)	19.0(7)
O33	3756(3)	5812(3)	1020(3)	19.6(7)
O121	6418(3)	5001(3)	4195(3)	18.7(7)
O231	6025(3)	4999(3)	1826(3)	13.2(6)

Table S23: Anisotropic Displacement Parameters ($Å^2 \times 10^3$) for $[Te_4][HS_3O_{10}]_2$. The anisotropic displacement factor exponent takes the form: $-2\pi^2[h^2a^{*2}U_{11}+2hka^*b^*U_{12}+\ldots]$.

Atom	U_{11}	U_{22}	U_{33}	U_{23}	U_{13}	U_{12}
Te1	10.03(14)	15.39(13)	14.48(15)	4.99(10)	-0.26(10)	-2.57(10)
Te2	10.61(14)	16.99(14)	13.78(15)	5.43(11)	-2.47(10)	-1.2(1)
S1	12.7(5)	14.7(5)	15.3(5)	-0.6(4)	-1.6(4)	2.4(4)
S2	13.6(5)	17.8(5)	15.6(5)	-0.7(4)	-1.5(4)	0.6(4)
S3	11.0(5)	11.7(4)	15.3(5)	-3.5(4)	-1.0(4)	0.4(4)
O11	19.3(17)	21.8(16)	21.1(18)	0.3(13)	5.1(14)	0.0(13)
O12	20.6(18)	16.1(15)	22.7(18)	-3.6(13)	0.1(14)	2.4(13)
O13	21.6(18)	20.0(16)	17.1(17)	1.7(13)	0.4(14)	2.4(13)
O21	13.4(16)	32.1(18)	21.6(18)	4.2(14)	4.4(14)	-5.9(14)
O22	23.0(18)	17.3(15)	27.0(19)	0.1(14)	-5.5(15)	4.0(14)
O31	24.5(19)	19.9(16)	20.8(18)	-11.3(14)	-1.4(14)	4.1(14)
O32	23.1(18)	12.8(14)	21.8(17)	-1.5(13)	6.0(14)	-2.7(13)
O33	13.2(16)	17.3(15)	26.1(18)	1.1(14)	-7.8(14)	-0.5(12)
O121	12.0(15)	26.3(16)	16.9(16)	-4.1(13)	-1.8(13)	4.7(13)
O231	12.1(14)	13.5(13)	14.3(15)	-2.9(12)	2.0(12)	4.0(12)

Table S24: Bond Lengths for $[Te_4][HS_3O_{10}]_2$ in pm.

Atom	Atom	Length/pm	Atom	Atom	Length/pm
Te1	Te2	266.68(4)	S2	O22	141.0(3)
Te1	Te2[1]	266.99(4)	S2	O121	161.7(3)
S1	O11	141.7(4)	S2	O231	156.7(3)
S1	O12	141.4(3)	S3	O31	142.5(3)
S1	O13	152.1(3)	S3	O32	143.6(4)
S1	O121	163.7(3)	S3	O33	142.8(3)
S2	O21	140.6(4)	S3	O231	170.9(3)

[1]-X, 1-Y, -Z

Table S25: Bond Angles for $[Te_4][HS_3O_{10}]_2$.

Atom	Atom	Atom	Angle/°	Atom	Atom	Atom	Angle/°
Te2	Te1	Te2[1]	90.546(12)	O22	S2	O121	109.28(19)
Te1	Te2	Te1[1]	89.454(12)	O22	S2	O231	106.3(2)
O11	S1	O13	111.2(2)	O231	S2	O121	101.39(18)
O11	S1	O121	108.94(19)	O31	S3	O32	116.9(2)
O12	S1	O11	121.1(2)	O31	S3	O33	115.9(2)
O12	S1	O13	109.7(2)	O31	S3	O231	103.71(18)
O12	S1	O121	102.07(19)	O32	S3	O231	97.90(18)
O13	S1	O121	101.72(19)	O33	S3	O32	114.8(2)
O21	S2	O22	122.2(2)	O33	S3	O231	104.01(17)
O21	S2	O121	104.1(2)	S2	O121	S1	123.0(2)
O21	S2	O231	111.54(19)	S2	O231	S3	123.0(2)

[1]-X, 1-Y, -Z

Table S26: Torsion Angles for $[Te_4][HS_3O_{10}]_2$.

A	B	C	D	Angle/°	A	B	C	D	Angle/°
O11	S1	O121	S2	36.7(3)	O22	S2	O231	S3	169.7(2)
O12	S1	O121	S2	165.8(3)	O31	S3	O231	S2	57.0(3)
O13	S1	O121	S2	-80.9(3)	O32	S3	O231	S2	177.3(2)
O21	S2	O121	S1	161.5(3)	O33	S3	O231	S2	-64.6(3)
O21	S2	O231	S3	34.2(3)	O121	S2	O231	S3	-76.1(2)
O22	S2	O121	S1	29.4(3)	O231	S2	O121	S1	-82.6(3)

Table S27: Hydrogen Atom Coordinates ($Å \times 10^4$) and Isotropic Displacement Parameters ($Å^2 \times 10^3$) for $[Te_4][HS_3O_{10}]_2$.

Atom	*x*	*y*	*z*	U(eq)
H13	7600.73	3776.55	6001.36	30

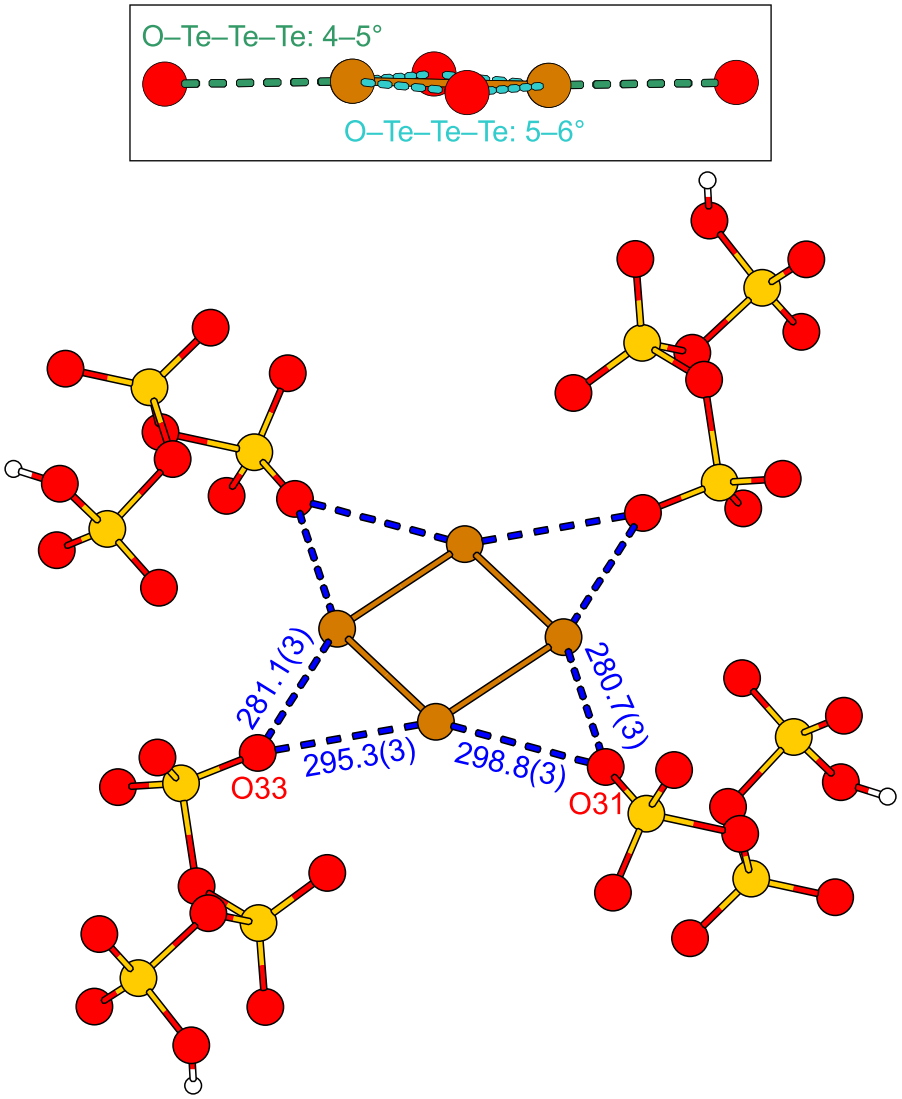

Figure S 14: Chalcogen-bonding (D–A distance below 300 pm) within $[Te_4][HS_3O_{10}]_2$. Distances are given in pm. O–Te coordination within the $[Te_4]$ plane and O–Te–Te–Te torsion angles are shown above.

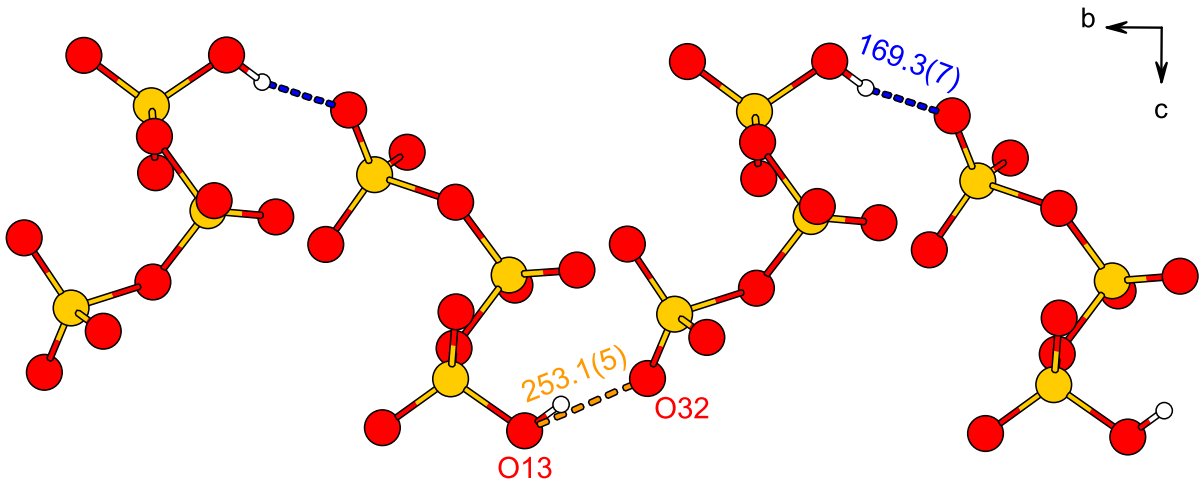

Figure S 15: Hydrogen-bonding within $[Te_4][HS_3O_{10}]_2$. Distances are given in pm.

$[Te_6][HS_3O_{10}]_4$-I (5)

Table S28: Crystallographic data of $[Te_6][HS_3O_{10}]_4$–I.

Empirical formula	$H_4O_{40}S_{12}Te_6$
Formula weight	1794.35 g/mol
Temperature	100.00 K
Crystal system	Triclinic
Space group	$P\bar{1}$ (No. 2)
Unit cell dimensions	a = 910.19(7) pm b = 1153.01(9) pm c = 1790.30(14) pm α = 99.888(3)° β = 94.994(3)° γ = 100.908(3)°
Volume	1803.6(2) Å^3
Z	2
ρ_{calc}	3.304 g/cm^3
μ	5.616 mm^{-1}
F(000)	1656
Crystal size	0.15 × 0.08 × 0.03 mm^3
Radiation	MoK_α (λ = 0.71073 nm)
2Θ range for data collection	4.592 to 63.012
Index ranges	-13 ≤ h ≤ 13, -16 ≤ k ≤ 16, -26 ≤ l ≤ 25
Reflections collected	64075
Independent reflections	11881 [R_{int} = 0.0504, R_σ = 0.0419]
Completeness	99.7%
Absorption correction	Multiscan
Min. and max. transmission	0.572 / 0.747
Data/restraints/parameters	11881/1/534
Goodness-of-fit on F^2	1.174
Final R indexes [I≥2σ (I)]	R_1 = 0.0573, wR_2 = 0.1205
Final R indexes [all data]	R_1 = 0.0700, wR_2 = 0.1251
Largest diff. peak/hole	2.28/–2.34 e · Å^{-3}

CCDC-No.	2476929

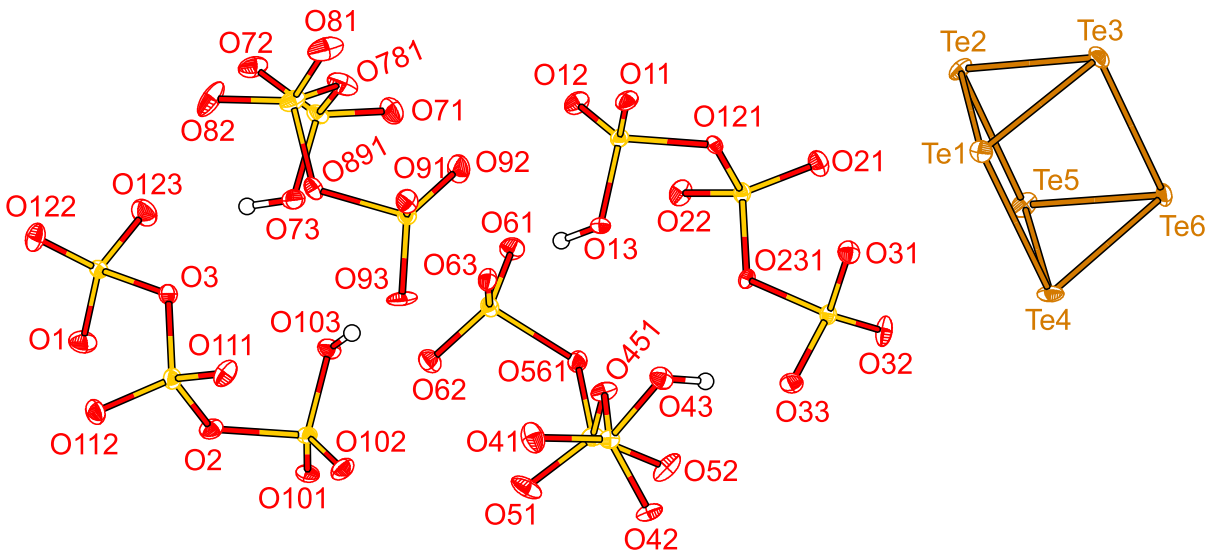

Figure S16: Thermal ellipsoid plot of the asymmetric unit of $[Te_6][HS_3O_{10}]_4$–I shown with 50% probability.

Table S29: Fractional Atomic Coordinates ($\times 10^4$) and Equivalent Isotropic Displacement Parameters ($Å^2 \times 10^3$) for $[Te_6][HS_3O_{10}]_4$–I. U_{eq} is defined as 1/3 of the trace of the orthogonalised U_{IJ} tensor.

Atom	*x*	*y*	*z*	U(eq)
Te1	9141.3(6)	5912.5(5)	2934.0(3)	12.53(10)
Te2	11245.2(6)	7906.6(5)	3549.2(3)	13.51(10)
Te3	11591.5(6)	6543.2(5)	2214.6(3)	14.13(11)
Te4	7449.7(6)	7600.5(5)	2036.6(3)	14.78(11)
Te5	9628.8(6)	9506.8(5)	2714.3(3)	15.17(11)
Te6	9967.6(6)	8204.5(5)	1367.9(3)	15.29(11)
S1	8156(2)	6953.3(17)	6320.7(10)	9.6(3)
S2	8222(2)	8434.2(17)	5188.1(10)	9.7(3)
S3	5952(2)	7202.7(16)	3937.0(10)	9.0(3)
O11	8463(6)	5800(5)	6263(3)	13.2(11)
O12	8948(7)	7928(5)	6899(3)	15.0(11)
O13	6472(6)	6920(6)	6227(3)	12.7(11)
O21	9153(7)	8598(5)	4605(3)	15.6(11)
O22	8286(7)	9377(5)	5827(3)	14.2(11)
O31	6871(7)	6319(5)	3860(3)	13.7(11)
O32	6213(7)	8096(5)	3467(3)	15.6(11)
O33	4393(6)	6765(5)	4022(3)	15.1(11)

O121	8571(6)	7285(5)	5478(3)	8.7(9)
O231	6534(6)	8027(5)	4850(3)	10.9(10)
S4	2429(2)	6352.5(17)	5453.2(11)	10.0(3)
S5	3302(2)	8908.8(17)	5843.5(11)	11.1(3)
S6	5455(2)	9621.3(17)	7227.1(11)	10.3(3)
S7	7864(2)	8676.0(17)	9265.2(11)	11.7(3)
S8	7104(2)	6144.1(18)	9303.2(12)	14.1(4)
S9	5255(2)	5386.1(17)	7860.6(10)	9.7(3)
O41	1968(7)	5926(6)	6108(4)	19.8(13)
O42	1362(6)	6596(5)	4899(3)	14.6(11)
O43	3495(7)	5590(5)	5099(3)	14.5(11)
O51	2099(7)	8937(6)	6293(4)	19.7(13)
O52	3179(8)	9219(6)	5112(4)	20.0(13)
O61	6894(6)	10410(5)	7271(3)	16.1(11)
O62	4361(7)	10065(5)	7643(3)	15.4(11)
O63	5500(6)	8374(5)	7215(3)	14.0(11)
O71	8427(7)	9169(6)	8656(4)	20.1(13)
O72	8575(7)	9069(6)	10025(4)	17.8(12)
O73	6173(6)	8562(5)	9219(3)	14.1(11)
O81	7853(8)	5190(6)	9074(4)	23.0(14)
O82	6900(9)	6500(6)	10075(4)	23.2(14)
O91	5068(7)	4110(5)	7788(3)	14.7(11)
O92	6545(7)	5981(6)	7591(4)	20.0(13)
O93	3857(6)	5772(5)	7691(4)	16.6(12)
O451	3706(6)	7597(5)	5757(3)	11.6(10)
O561	4847(6)	9610(5)	6270(3)	12.1(10)
O781	8021(7)	7257(5)	9005(4)	18.8(12)
O891	5521(6)	5902(5)	8829(3)	11.3(10)
S10	1636(2)	7686.0(18)	8310.3(11)	11.1(3)
S11	1636(2)	6459.4(17)	9579.5(11)	11.5(3)
S12	3876(2)	8085.1(17)	10716.6(11)	10.9(3)
O1	2722(7)	8769(6)	10704(4)	18.5(12)
O2	1270(7)	7523(5)	9175(3)	14.5(11)

O3	3319(6)	6939(5)	9913(3)	11.6(10)
O101	1351(7)	8841(6)	8295(3)	17.0(12)
O102	811(7)	6649(6)	7796(3)	16.6(12)
O103	3317(6)	7732(5)	8373(3)	14.0(11)
O111	1601(7)	5424(6)	9024(3)	18.1(12)
O112	690(7)	6448(6)	10170(3)	16.1(11)
O122	3947(7)	7430(6)	11324(3)	17.4(12)
O123	5300(7)	8636(6)	10527(4)	21.9(13)

Table S30: Anisotropic Displacement Parameters ($Å^2 \times 10^3$) for $[Te_6][HS_3O_{10}]_4$–I. The anisotropic displacement factor exponent takes the form: $-2\pi^2[h^2a^{*2}U_{11}+2hka^*b^*U_{12}+\ldots]$.

Atom	U_{11}	U_{22}	U_{33}	U_{23}	U_{13}	U_{12}
Te1	12.5(2)	9.5(2)	15.9(2)	5.21(18)	2.75(18)	0.15(17)
Te2	16.0(2)	12.5(2)	9.8(2)	0.46(17)	-4.82(18)	1.96(18)
Te3	14.2(2)	16.8(2)	15.3(2)	4.64(19)	7.12(18)	9.00(19)
Te4	6.4(2)	17.0(2)	21.0(3)	7.9(2)	-1.16(18)	0.00(18)
Te5	21.4(3)	7.6(2)	14.9(2)	-1.13(18)	-3.05(19)	4.37(19)
Te6	17.3(2)	23.4(3)	10.3(2)	8.07(19)	7.06(18)	10.2(2)
S1	10.0(7)	9.9(8)	8.6(8)	0.3(6)	0.0(6)	2.9(6)
S2	11.1(8)	8.8(8)	8.0(7)	-0.1(6)	1.4(6)	0.5(6)
S3	11.2(8)	7.8(8)	7.8(7)	0.7(6)	1.4(6)	1.9(6)
O11	15(3)	13(3)	13(3)	3(2)	-1(2)	7(2)
O12	16(3)	12(3)	14(3)	-1(2)	-3(2)	1(2)
O13	7(2)	20(3)	11(3)	2(2)	0.0(19)	3(2)
O21	15(3)	16(3)	14(3)	0(2)	5(2)	-1(2)
O22	20(3)	7(2)	12(3)	-4(2)	-1(2)	1(2)
O31	16(3)	12(3)	14(3)	2(2)	3(2)	5(2)
O32	30(3)	11(3)	8(2)	2(2)	5(2)	7(2)
O33	9(2)	18(3)	14(3)	-1(2)	-1(2)	-1(2)
O121	9(2)	8(2)	9(2)	0.8(19)	2.8(18)	3.2(18)
O231	11(2)	13(3)	6(2)	-3.1(19)	-0.9(19)	2(2)
S4	9.9(7)	8.3(8)	11.5(8)	1.5(6)	0.7(6)	1.9(6)
S5	10.6(8)	8.5(8)	13.1(8)	0.0(6)	-0.9(6)	2.4(6)

S6	10.1(7)	9.8(8)	10.0(8)	0.2(6)	2.3(6)	0.6(6)
S7	7.7(7)	11.2(8)	14.5(8)	0.8(7)	1.9(6)	-0.6(6)
S8	15.4(9)	10.2(8)	14.1(9)	-1.9(7)	-4.4(7)	2.6(7)
S9	8.6(7)	9.8(8)	10.0(8)	0.8(6)	0.7(6)	1.9(6)
O41	26(3)	16(3)	21(3)	7(2)	10(3)	6(2)
O42	11(2)	16(3)	16(3)	4(2)	-5(2)	2(2)
O43	15(3)	12(3)	16(3)	0(2)	3(2)	5(2)
O51	11(3)	15(3)	29(3)	-8(2)	5(2)	3(2)
O52	27(3)	17(3)	14(3)	4(2)	-8(2)	2(2)
O61	11(3)	16(3)	18(3)	3(2)	0(2)	-3(2)
O62	14(3)	16(3)	16(3)	0(2)	4(2)	3(2)
O63	14(3)	18(3)	10(2)	4(2)	2(2)	2(2)
O71	17(3)	24(3)	19(3)	6(3)	7(2)	2(2)
O72	14(3)	15(3)	20(3)	-3(2)	-6(2)	1(2)
O73	12(2)	16(3)	15(3)	3(2)	0(2)	4(2)
O81	23(3)	13(3)	28(3)	-6(2)	-10(3)	7(2)
O82	44(4)	11(3)	11(3)	-2(2)	-8(3)	7(3)
O91	15(3)	13(3)	13(3)	-3(2)	1(2)	1(2)
O92	17(3)	24(3)	16(3)	5(2)	4(2)	-5(2)
O93	11(3)	15(3)	22(3)	-3(2)	-7(2)	8(2)
O451	12(2)	5(2)	16(3)	-0.2(19)	-4(2)	0.6(19)
O561	13(2)	13(3)	10(2)	1(2)	1(2)	2(2)
O781	12(3)	14(3)	28(3)	-3(2)	3(2)	2(2)
O891	12(2)	9(2)	13(3)	1(2)	5(2)	1.0(19)
S10	9.8(8)	13.3(8)	11.0(8)	2.0(6)	0.0(6)	5.4(6)
S11	12.4(8)	12.0(8)	9.2(8)	0.6(6)	1.5(6)	1.8(6)
S12	8.4(7)	13.3(8)	10.7(8)	2.3(6)	2.0(6)	1.2(6)
O1	17(3)	17(3)	23(3)	3(2)	2(2)	9(2)
O2	16(3)	14(3)	14(3)	1(2)	-1(2)	8(2)
O3	12(2)	13(3)	9(2)	-2(2)	1.0(19)	4(2)
O101	14(3)	24(3)	16(3)	3(2)	2(2)	13(2)
O102	17(3)	20(3)	11(3)	-1(2)	-4(2)	5(2)
O103	11(2)	14(3)	15(3)	-3(2)	1(2)	3(2)

O111	22(3)	17(3)	12(3)	1(2)	-3(2)	2(2)
O112	15(3)	19(3)	14(3)	5(2)	6(2)	1(2)
O122	23(3)	17(3)	12(3)	7(2)	3(2)	1(2)
O123	15(3)	26(3)	21(3)	1(3)	5(2)	-2(2)

Table S31: Bond Lengths for $[Te_6][HS_3O_{10}]_4$–I in pm.

Atom	Atom	Length/pm	Atom	Atom	Length/pm
Te1	Te2	269.50(8)	S6	O61	143.3(6)
Te1	Te3	271.46(7)	S6	O62	141.4(6)
Te1	Te4	324.30(8)	S6	O63	144.3(6)
Te2	Te3	270.34(8)	S6	O561	175.1(6)
Te2	Te5	306.51(8)	S7	O71	140.6(6)
Te3	Te6	313.53(8)	S7	O72	141.4(6)
Te4	Te5	269.30(8)	S7	O73	151.3(6)
Te4	Te6	270.75(8)	S7	O781	165.9(6)
Te5	Te6	268.72(8)	S8	O81	142.2(6)
S1	O11	139.8(6)	S8	O82	141.0(7)
S1	O12	142.1(6)	S8	O781	159.2(7)
S1	O13	152.0(6)	S8	O891	155.8(6)
S1	O121	167.5(6)	S9	O91	143.1(6)
S2	O21	141.6(6)	S9	O92	141.0(6)
S2	O22	142.5(6)	S9	O93	145.1(6)
S2	O121	157.9(6)	S9	O891	171.4(6)
S2	O231	155.4(6)	S10	O2	164.6(6)
S3	O31	143.2(6)	S10	O101	140.8(6)
S3	O32	143.7(6)	S10	O102	141.5(6)
S3	O33	144.3(6)	S10	O103	151.5(6)
S3	O231	172.6(6)	S11	O2	159.8(6)
S4	O41	141.4(6)	S11	O3	155.4(6)
S4	O42	142.7(6)	S11	O111	141.0(6)
S4	O43	153.4(6)	S11	O112	142.0(6)
S4	O451	164.2(6)	S12	O1	142.8(6)
S5	O51	141.6(6)	S12	O3	174.4(6)

S5	O52	141.7(6)	S12	O122	143.0(6)
S5	O451	160.8(6)	S12	O123	142.8(7)

Table S32: Bond Angles for $[Te_6][HS_3O_{10}]_4$–I.

Atom	Atom	Atom	Angle/°	Atom	Atom	Atom	Angle/°
Te2	Te1	Te3	59.96(2)	O561	S5	O451	96.1(3)
Te2	Te1	Te4	87.36(2)	O61	S6	O63	115.2(4)
Te3	Te1	Te4	88.62(2)	O61	S6	O561	97.0(3)
Te1	Te2	Te3	60.38(2)	O62	S6	O61	117.5(4)
Te1	Te2	Te5	92.65(2)	O62	S6	O63	115.8(4)
Te3	Te2	Te5	91.74(2)	O62	S6	O561	105.0(3)
Te1	Te3	Te6	91.25(2)	O63	S6	O561	102.2(3)
Te2	Te3	Te1	59.66(2)	O71	S7	O72	122.1(4)
Te2	Te3	Te6	87.98(2)	O71	S7	O73	110.7(4)
Te5	Te4	Te1	88.86(2)	O71	S7	O781	100.7(4)
Te5	Te4	Te6	59.68(2)	O72	S7	O73	111.9(4)
Te6	Te4	Te1	89.09(2)	O72	S7	O781	106.5(4)
Te4	Te5	Te2	91.13(2)	O73	S7	O781	102.3(3)
Te6	Te5	Te2	89.74(2)	O81	S8	O781	104.4(4)
Te6	Te5	Te4	60.43(2)	O81	S8	O891	110.4(3)
Te4	Te6	Te3	91.02(2)	O82	S8	O81	121.1(4)
Te5	Te6	Te3	90.53(2)	O82	S8	O781	109.8(4)
Te5	Te6	Te4	59.89(2)	O82	S8	O891	106.7(4)
O11	S1	O12	121.6(4)	O891	S8	O781	103.0(3)
O11	S1	O13	111.9(4)	O91	S9	O93	113.4(4)
O11	S1	O121	101.5(3)	O91	S9	O891	103.6(3)
O12	S1	O13	111.8(3)	O92	S9	O91	116.5(4)
O12	S1	O121	107.3(3)	O92	S9	O93	116.9(4)
O13	S1	O121	99.5(3)	O92	S9	O891	105.1(3)
O21	S2	O22	120.9(4)	O93	S9	O891	98.1(3)
O21	S2	O121	105.2(3)	S5	O451	S4	122.4(3)
O21	S2	O231	111.0(3)	S5	O561	S6	124.3(4)
O22	S2	O121	109.5(3)	S8	O781	S7	125.0(4)

O22	S2	O231	106.0(3)	S8	O891	S9	121.8(3)
O231	S2	O121	102.9(3)	O101	S10	O2	101.3(3)
O31	S3	O32	116.2(4)	O101	S10	O102	122.1(4)
O31	S3	O33	115.8(4)	O101	S10	O103	110.0(4)
O31	S3	O231	104.1(3)	O102	S10	O2	107.2(4)
O32	S3	O33	115.5(4)	O102	S10	O103	111.9(3)
O32	S3	O231	103.1(3)	O103	S10	O2	101.6(3)
O33	S3	O231	98.4(3)	O3	S11	O2	102.3(3)
S2	O121	S1	123.3(3)	O111	S11	O2	110.0(3)
S2	O231	S3	122.7(3)	O111	S11	O3	106.0(3)
O41	S4	O42	121.0(4)	O111	S11	O112	122.0(4)
O41	S4	O43	108.7(4)	O112	S11	O2	103.8(3)
O41	S4	O451	106.9(4)	O112	S11	O3	111.1(3)
O42	S4	O43	113.2(4)	O1	S12	O3	104.1(3)
O42	S4	O451	107.3(3)	O1	S12	O122	116.1(4)
O43	S4	O451	96.7(3)	O122	S12	O3	102.4(3)
O51	S5	O52	120.0(4)	O123	S12	O1	116.2(4)
O51	S5	O451	108.5(4)	O123	S12	O3	99.2(3)
O51	S5	O561	113.8(3)	O123	S12	O122	115.2(4)
O52	S5	O451	108.6(4)	S11	O2	S10	124.8(4)
O52	S5	O561	107.2(4)	S11	O3	S12	122.1(3)

Table S33: Torsion Angles for $[Te_6][HS_3O_{10}]_4$–I.

A	B	C	D	Angle/°	A	B	C	D	Angle/°
O11	S1	O121	S2	171.6(4)	O73	S7	O781	S8	-44.9(6)
O12	S1	O121	S2	-59.8(5)	O81	S8	O781	S7	-166.7(5)
O13	S1	O121	S2	56.8(5)	O81	S8	O891	S9	-43.9(5)
O21	S2	O121	S1	161.5(4)	O82	S8	O781	S7	-35.5(6)
O21	S2	O231	S3	29.2(5)	O82	S8	O891	S9	-177.2(4)
O22	S2	O121	S1	30.1(5)	O91	S9	O891	S8	84.7(5)
O22	S2	O231	S3	162.2(4)	O92	S9	O891	S8	-37.9(5)
O31	S3	O231	S2	42.9(5)	O93	S9	O891	S8	-158.7(4)
O32	S3	O231	S2	-78.9(5)	O451	S5	O561	S6	-73.9(4)

O33	S3	O231	S2	162.3(4)	O561	S5	O451	S4	170.4(4)
O121	S2	O231	S3	-82.9(4)	O781	S8	O891	S9	67.1(4)
O231	S2	O121	S1	-82.3(4)	O891	S8	O781	S7	77.9(5)
O41	S4	O451	S5	-96.8(5)	O1	S12	O3	S11	-27.7(5)
O42	S4	O451	S5	34.5(5)	O2	S11	O3	S12	74.2(4)
O43	S4	O451	S5	151.3(4)	O3	S11	O2	S10	83.7(5)
O51	S5	O451	S4	52.8(5)	O101	S10	O2	S11	-170.0(5)
O51	S5	O561	S6	39.4(6)	O102	S10	O2	S11	60.9(5)
O52	S5	O451	S4	-79.2(5)	O103	S10	O2	S11	-56.6(5)
O52	S5	O561	S6	174.5(4)	O111	S11	O2	S10	-28.6(6)
O61	S6	O561	S5	-179.3(4)	O111	S11	O3	S12	-170.5(4)
O62	S6	O561	S5	-58.3(5)	O112	S11	O2	S10	-160.6(4)
O63	S6	O561	S5	62.9(5)	O112	S11	O3	S12	-36.0(5)
O71	S7	O781	S8	-159.0(5)	O122	S12	O3	S11	93.6(5)
O72	S7	O781	S8	72.7(6)	O123	S12	O3	S11	-147.9(5)

Table S34: Hydrogen Atom Coordinates (Å×10^4) and Isotropic Displacement Parameters (Å^2×10^3) for $[Te_6][HS_3O_{10}]_4$–I.

Atom	***x***	***y***	***z***	**U(eq)**
H43	3740(140)	5890(100)	4720(50)	30(30)
H73	5950.39	8872.98	9642.15	30(30)
H103	3474.87	7068.7	8156.63	20(30)
H13	6210(140)	7430(120)	6580(70)	33

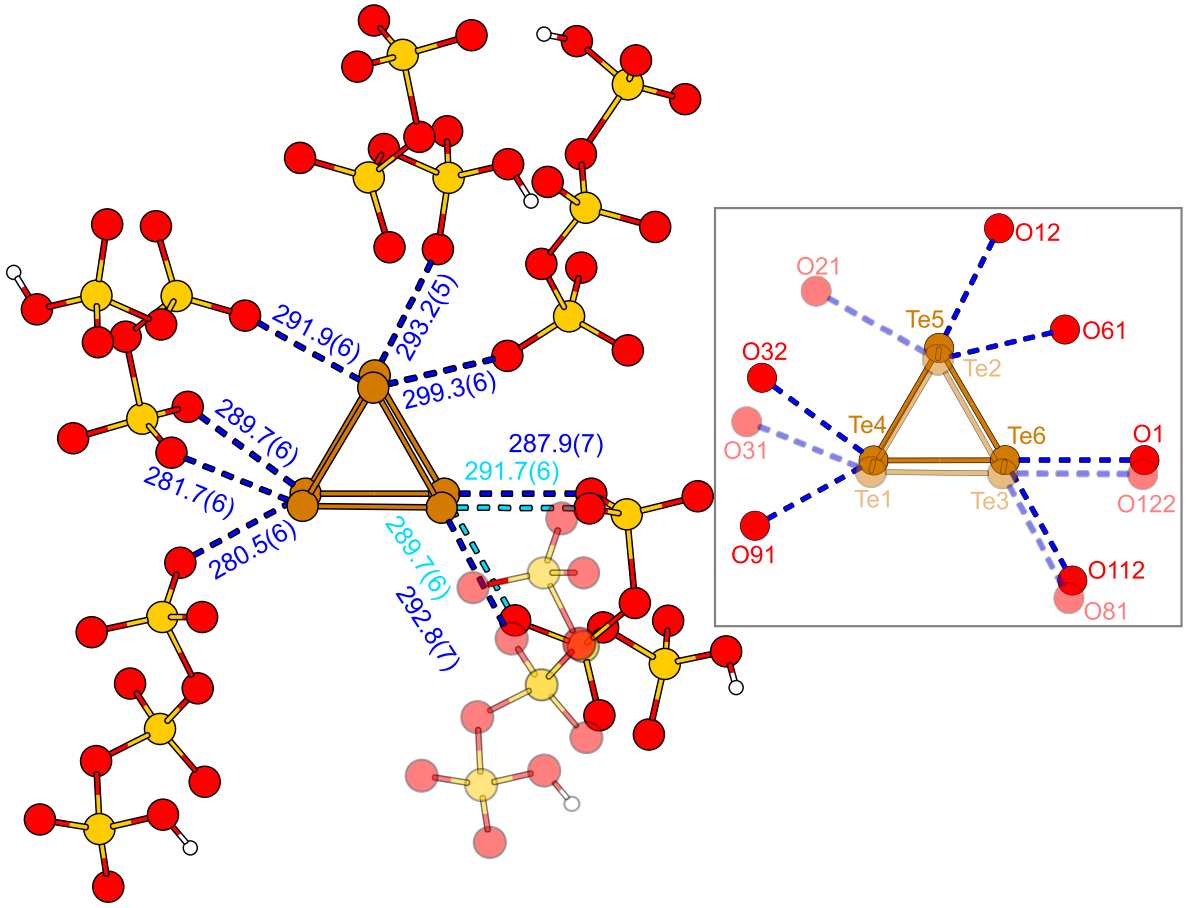

Figure S 17: Chalcogen-bonding (D–A distance below 300 pm) within $[Te_6][HS_3O_{10}]_4$–I. Distances are given in pm. O–Te coordination within the two $[Te_3]$ planes is shown in the right corner. In case of overlapping atoms, the atoms in the upper plane are shown at 50% visibility.

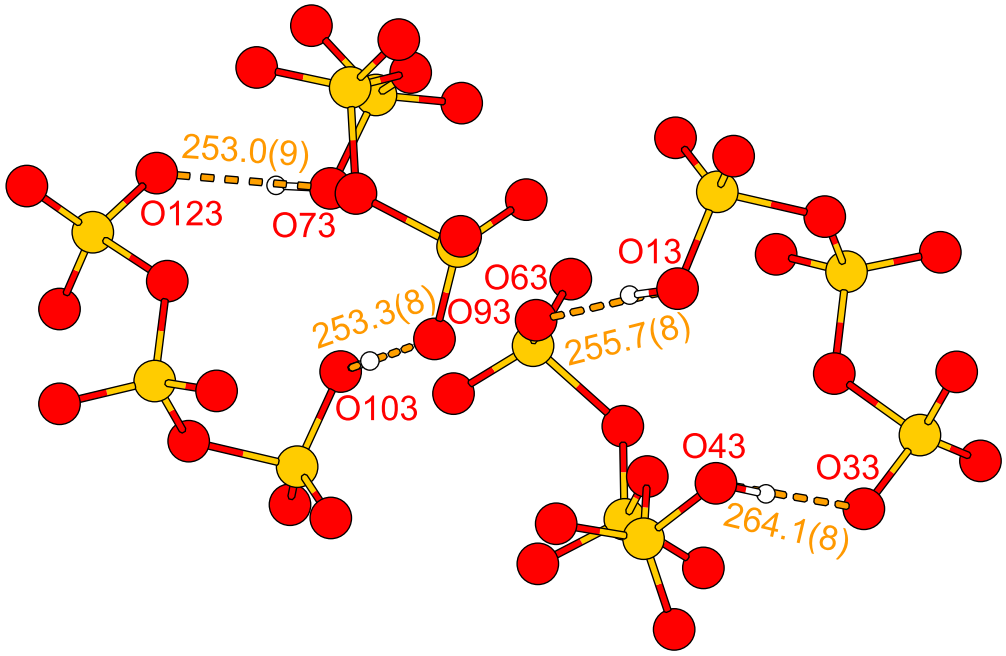

Figure S 18: Hydrogen-bonding Donor-Acceptor (O···O) distances within $[Te_6][HS_3O_{10}]_4$–I. Distances are given in pm.

$[Te_6][HS_3O_{10}]_4$-II (6)

Table S35: Crystallographic data of $[Te_6][HS_3O_{10}]_4$-II.

Empirical formula	$H_4O_{40}S_{12}Te_6$
Formula weight	3587.70 g/mol
Temperature	100.00 K
Crystal system	Triclinic
Space group	$P\bar{1}$ (No. 2)
Unit cell dimensions	a = 1342.99(7) pm
	b = 1516.05(7) pm
	c = 1993.31(10) pm
	α = 99.470(2)°
	β = 105.770(2)°
	γ = 105.953(2)°
Volume	3627.6(3) Å^3
Z	4
ρ_{calc}	3.285 g/cm^3
μ	5.585 mm^{-1}
F(000)	3310
Crystal size	0.06 × 0.04 × 0.01 mm^3
Radiation	MoK_α (λ = 0.71073 nm)
2Θ range for data collection	4.032 to 61.014
Index ranges	-19 ≤ h ≤ 19, -21 ≤ k ≤ 21, -28 ≤ l ≤ 28
Reflections collected	289588
Independent reflections	22166 [R_{int} = 0.0577, R_σ = 0.0265]
Completeness	100%
Absorption correction	Multiscan
Min. and max. transmission	0.655 / 0.747
Data/restraints/parameters	22166/3/1080
Goodness-of-fit on F^2	1.074
Final R indexes [I≥2σ (I)]	R_1 = 0.0379, wR_2 = 0.0921
Final R indexes [all data]	R_1 = 0.0471, wR_2 = 0.0962
Largest diff. peak/hole	3.68/–0.95 e · Å^{-3}

CCDC-No.	2476936

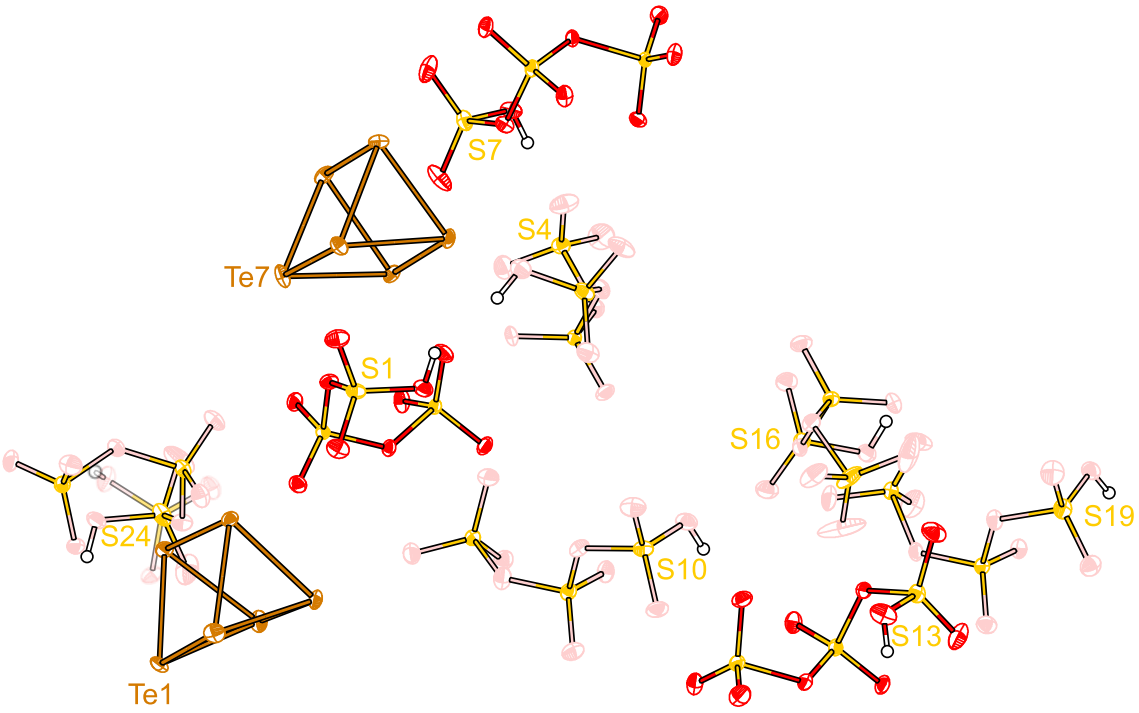

Figure S19: Thermal ellipsoid plot of the asymmetric unit of $[Te_6][HS_3O_{10}]_4$-II shown with 50% probability. For an improved contrast, half of the anions are colored differently. The disordered minor fraction (0.33) of the terminal SO_3H unit (S24) is shown at 50% visibility.

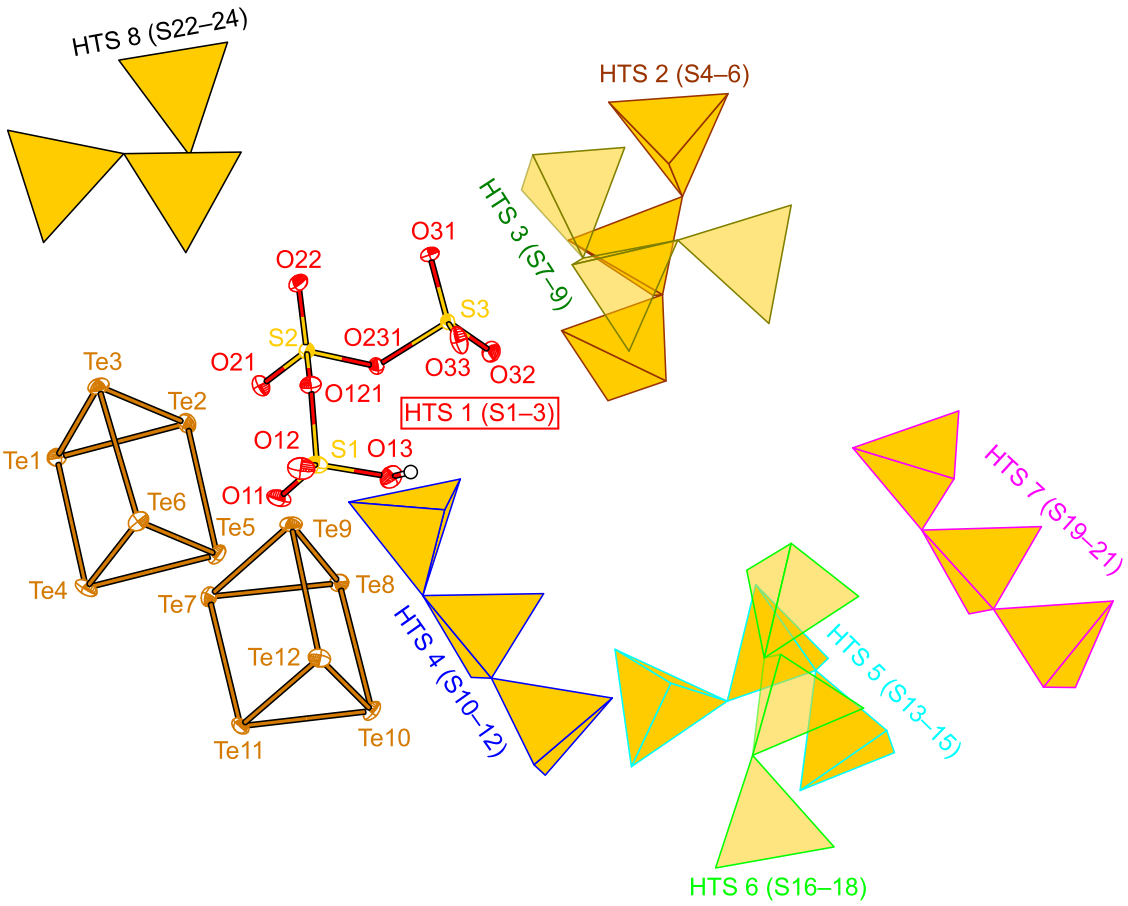

Figure S 20: Asymmetric unit of $[Te_6][HS_3O_{10}]_4$-II. For differentiation, the hydrogentrisulfate (HTS) anions are shown as polyhedral, except for HTS1 which is shown as thermal ellipsoid plot (50% probability). In case of overlying anion, the anion in the upper plane is shown at 50% visibility.

Table S36: Fractional Atomic Coordinates ($\times 10^4$) and Equivalent Isotropic Displacement Parameters ($Å^2 \times 10^3$) for $[Te_6][HS_3O_{10}]_4$-II. Ueq is defined as 1/3 of the trace of the orthogonalised U_{IJ} tensor.

Atom	*x*	*y*	*z*	U(eq)
Te1	3559.6(3)	1748.3(2)	-27.8(2)	14.92(6)
Te2	4921.1(3)	2181.8(3)	1354.5(2)	16.34(7)
Te3	4727.5(3)	3562.9(2)	681.9(2)	15.43(7)
Te4	1655.1(3)	1889.3(2)	540.1(2)	18.08(7)
Te5	3030.6(3)	2169.5(2)	1895.9(2)	14.04(6)
Te6	2826.1(3)	3655.8(2)	1354.3(2)	13.85(6)
Te7	1633.6(3)	7063.9(3)	2974.5(2)	17.92(7)
Te8	2763.6(3)	6827.2(2)	4244.6(2)	13.50(6)
Te9	3134.6(3)	8573.5(2)	4032.5(2)	15.58(7)
Te10	920.1(3)	7027.5(2)	4853.7(2)	15.28(7)
Te11	-229.6(2)	7186.5(2)	3556.4(2)	13.88(6)
Te12	1171.4(3)	8742.0(2)	4599.4(2)	14.82(6)

S1	4705.5(10)	5325.9(8)	3472.7(7)	14.0(2)
S2	6502.7(9)	4957.0(8)	3082.8(6)	10.55(19)
S3	7897.4(9)	5087.2(8)	4518.5(6)	10.31(19)
O11	4032(3)	4457(3)	2944(2)	19.4(7)
O12	4423(3)	6159(3)	3500(2)	21.7(8)
O13	5026(3)	5174(3)	4226(2)	18.7(7)
O21	5744(3)	4189(3)	2500.3(19)	15.4(7)
O22	7439(3)	5586(3)	3015.3(19)	15.4(7)
O31	8811(3)	5359(3)	4275(2)	18.7(7)
O32	7818(3)	4317(3)	4849(2)	16.8(7)
O33	7578(3)	5839(3)	4836(2)	19.9(8)
O121	5890(3)	5653(2)	3338.6(19)	13.5(6)
O231	6789(3)	4519(2)	3732.2(18)	12.3(6)
S4	8303.8(10)	6360.8(9)	6692.5(7)	16.6(2)
S5	10097.8(9)	5844.5(8)	6523.6(6)	11.6(2)
S6	12132.3(10)	7438.6(9)	7000.8(7)	15.1(2)
O41	7681(3)	5379(3)	6384(2)	21.9(8)
O42	8181(3)	6902(3)	7289(2)	25.4(9)
O43	8280(3)	6914(3)	6122(2)	20.2(8)
O51	9730(3)	4885(2)	6555(2)	18.3(7)
O52	9881(3)	6058(3)	5842.6(18)	13.0(6)
O61	13090(4)	7517(3)	7559(3)	33.7(11)
O62	12176(4)	7305(3)	6291(2)	27.7(9)
O63	11504(4)	8009(3)	7180(3)	29.8(10)
O451	9591(3)	6447(3)	6998.3(19)	15.9(7)
O561	11308(3)	6303(3)	6999.8(19)	15.2(7)
S7	10270.0(11)	9502.7(9)	6413.5(7)	16.9(2)
S8	8961.8(9)	9962.7(8)	7261.4(6)	11.6(2)
S9	10310.3(9)	9827.3(8)	8627.9(6)	10.32(19)
O71	10396(4)	10409(3)	6284(2)	25.8(9)
O72	9996(4)	8694(3)	5848(2)	28.9(9)
O73	11251(3)	9583(3)	7044(2)	17.6(7)
O81	8869(3)	10731(3)	6961(2)	16.8(7)

O82	8068(3)	9365(3)	7399(2)	16.9(7)
O91	11323(3)	10530(3)	9077(2)	17.6(7)
O92	9398(3)	9736(3)	8882(2)	17.5(7)
O93	10378(3)	8950(2)	8269.7(19)	16.3(7)
O781	9257(3)	9228(2)	6731.1(19)	15.2(7)
O891	10026(3)	10367(2)	7932.0(18)	12.0(6)
S10	2406.1(10)	1806.5(9)	5564.2(7)	15.4(2)
S11	3666.3(9)	1503.2(8)	4672.4(7)	13.3(2)
S12	5007.8(10)	2745.1(8)	4031.7(7)	15.5(2)
O1	5845(3)	2364(3)	4320(2)	20.6(8)
O10B	2924(3)	2066(2)	4931(2)	16.2(7)
O11B	3797(3)	1939(3)	4046(2)	20.5(8)
O101	1912(3)	803(3)	5376(2)	21.2(8)
O102	1785(3)	2420(3)	5599(2)	22.8(8)
O103	3412(3)	2153(3)	6239(2)	20.0(8)
O111	3007(3)	535(3)	4377(2)	20.3(8)
O112	4665(3)	1763(3)	5253(2)	16.9(7)
O122	4683(3)	2682(3)	3280(2)	23.0(8)
O123	5077(4)	3612(3)	4493(2)	24.9(9)
S13	4619.3(10)	401.9(9)	8445.5(7)	14.4(2)
S14	5654.2(10)	-61.4(8)	7415.0(6)	12.5(2)
S15	3968.4(10)	-106.4(8)	6147.4(7)	15.7(2)
O13B	5423(3)	689(2)	7966.5(19)	13.7(6)
O14B	4510(3)	-574(2)	6825.7(19)	15.5(7)
O131	4793(4)	-369(3)	8692(3)	27.6(9)
O132	4867(4)	1292(3)	8940(2)	25.7(9)
O133	3492(3)	108(3)	7890(2)	24.7(8)
O141	5903(3)	-761(3)	7754(2)	18.7(7)
O142	6406(3)	513(3)	7154(2)	17.4(7)
O151	2839(3)	-698(3)	5921(2)	24.6(9)
O152	4537(4)	-236(3)	5648(2)	24.8(8)
O153	4220(3)	861(3)	6528(2)	19.4(8)
S16	6282.8(10)	3218.3(8)	8103.8(7)	14.3(2)

S17	4525.5(10)	3623.6(8)	8462.3(6)	12.9(2)
S18	2367.2(11)	2199.5(10)	8088.9(9)	26.9(3)
O16B	4959(3)	3021(2)	7931.1(18)	13.6(6)
O17B	3299(3)	3231(2)	8030(2)	15.9(7)
O161	6296(3)	2600(3)	7502(2)	23.0(8)
O162	6803(3)	4211(3)	8272(2)	20.4(8)
O163	6602(3)	2846(3)	8761(2)	17.8(7)
O171	4780(3)	3377(3)	9126.0(19)	15.7(7)
O172	4907(3)	4591(3)	8445(2)	19.9(8)
O181	2765(4)	1493(3)	7797(4)	60(2)
O182	1392(3)	2269(3)	7633(3)	30.2(10)
O183	2509(4)	2375(4)	8844(3)	46.4(15)
S19	7249.6(10)	1408.2(9)	10629.0(7)	16.4(2)
S20	8166.4(9)	882.2(8)	9578.9(6)	11.6(2)
S21	9318.6(11)	2417.8(9)	9074.1(7)	16.2(2)
O19B	7487(3)	1485(3)	9875.7(19)	15.7(7)
O20B	8287(3)	1328(3)	8957.5(19)	14.6(7)
O191	6521(3)	1930(3)	10629(2)	24.7(8)
O192	6935(3)	431(3)	10623(2)	21.7(8)
O193	8355(3)	1979(3)	11207(2)	19.3(7)
O201	7461(3)	-75(3)	9283(2)	18.5(7)
O202	9181(3)	1105(3)	10140.6(19)	14.1(7)
O211	8979(4)	2480(3)	8355(2)	31.3(10)
O212	9086(4)	3046(3)	9585(2)	29.9(10)
O213	10315(3)	2224(3)	9329(3)	27.5(9)
S22	7348.9(10)	5092.6(8)	141.9(7)	14.8(2)
S23	8370.8(10)	5012.6(9)	1584.5(6)	13.5(2)
S24	10161.8(10)	4529.0(10)	1302.7(7)	18.3(2)
O22B	8329(3)	5546(3)	975.1(19)	16.8(7)
O23B	8921(3)	4248(3)	1370(2)	16.3(7)
O23T	7318(3)	4460(3)	1550(2)	19.9(8)
O221	7258(3)	4109(3)	-19(2)	17.9(7)
O222	6406(3)	5282(3)	241(2)	22.2(8)

O223	7904(3)	5663(3)	-242(2)	22.2(8)
O232	9123(3)	5703(3)	2221(2)	20.5(8)
O241	9904(5)	4641(4)	555(3)	17.7(11)
O242	10895(9)	4833(9)	2011(6)	20(2)
O243	10158(9)	3649(7)	902(7)	15(2)
O244	10261(9)	5265(9)	886(7)	20(2)
O245	10830(5)	5355(6)	1806(4)	33.8(17)
O246	10363(6)	3634(5)	1323(5)	34.6(17)

Table S37: Anisotropic Displacement Parameters ($Å^2 \times 10^3$) for $[Te_6][HS_3O_{10}]_4$-II. The anisotropic displacement factor exponent takes the form: $-2\pi^2[h^2a^{*2}U_{11}+2hka^*b^*U_{12}+\ldots]$.

Atom	U_{11}	U_{22}	U_{33}	U_{23}	U_{13}	U_{12}
Te1	15.37(14)	14.02(14)	11.24(14)	-2.54(11)	5.59(11)	0.89(11)
Te2	12.36(14)	25.07(16)	15.48(15)	8.03(12)	4.18(11)	11.07(12)
Te3	15.96(14)	11.45(13)	16.70(15)	2.81(11)	8.22(12)	-0.95(11)
Te4	8.52(13)	18.06(15)	20.28(16)	1.83(12)	-0.03(12)	-0.23(11)
Te5	17.97(15)	17.98(15)	14.07(14)	9.87(12)	9.88(12)	10.34(12)
Te6	18.29(15)	10.99(13)	16.65(15)	4.95(11)	9.40(12)	7.31(11)
Te7	15.91(15)	28.11(17)	8.77(14)	3.41(12)	4.94(11)	5.91(13)
Te8	12.86(13)	13.55(14)	17.54(15)	7.89(11)	6.09(11)	6.46(11)
Te9	11.46(13)	12.71(14)	23.16(16)	8.79(12)	6.88(12)	1.46(11)
Te10	19.31(15)	16.99(14)	13.44(14)	9.08(12)	8.99(12)	5.62(12)
Te11	8.21(13)	17.78(14)	11.46(14)	0.37(11)	0.86(10)	2.35(11)
Te12	13.97(14)	9.30(13)	19.18(15)	0.59(11)	5.42(12)	2.76(11)
S1	12.2(5)	12.0(5)	17.2(6)	1.2(4)	5.6(4)	4.2(4)
S2	10.9(5)	10.9(5)	9.5(5)	2.7(4)	3.5(4)	3.1(4)
S3	9.5(5)	10.9(5)	9.2(5)	4.1(4)	1.7(4)	2.0(4)
O11	11.1(16)	19.2(18)	22.2(19)	0.5(15)	4.7(14)	0.1(13)
O12	20.4(18)	17.1(18)	30(2)	4.6(16)	10.1(16)	9.2(15)
O13	24.0(19)	15.9(17)	16.8(18)	1.1(14)	9.8(15)	6.5(15)
O21	14.4(16)	15.4(16)	12.8(16)	1.6(13)	1.3(13)	4.0(13)
O22	16.0(16)	16.1(16)	14.8(17)	6.2(13)	7.6(13)	2.9(13)
O31	11.6(16)	28(2)	14.9(17)	8.7(15)	6.1(13)	0.1(14)
O32	18.9(17)	13.4(16)	16.1(17)	8.2(13)	3.4(14)	2.2(13)
O33	23.6(19)	20.2(18)	12.4(17)	-0.8(14)	-0.8(14)	11.5(15)
O121	13.6(15)	11.5(15)	17.6(17)	3.2(13)	7.5(13)	5.4(12)
O231	10.9(15)	12.6(15)	10.6(15)	4.8(12)	1.2(12)	0.9(12)
S4	14.9(5)	17.2(5)	16.1(6)	-0.6(4)	7.8(4)	3.1(4)
S5	12.6(5)	10.9(5)	10.6(5)	3.3(4)	3.8(4)	2.9(4)
S6	11.6(5)	13.5(5)	15.9(5)	2.0(4)	0.3(4)	2.9(4)
O41	20.1(18)	20.8(19)	23(2)	1.1(15)	13.1(16)	1.8(15)
O42	20.8(19)	27(2)	25(2)	-6.5(16)	13.9(17)	5.0(16)

O43	20.5(18)	20.4(18)	18.9(18)	2.6(15)	3.4(15)	10.1(15)
O51	25.1(19)	11.0(16)	22.0(19)	7.4(14)	12.4(16)	4.8(14)
O52	10.7(15)	19.6(17)	7.7(15)	4.1(13)	3.0(12)	3.6(13)
O61	20(2)	32(2)	31(2)	5.8(19)	-9.2(18)	0.0(17)
O62	27(2)	26(2)	19(2)	5.0(16)	7.3(17)	-6.8(17)
O63	29(2)	17.7(19)	48(3)	8.7(19)	20(2)	10.5(17)
O451	15.5(16)	20.2(17)	13.2(16)	3.1(13)	6.5(13)	6.8(14)
O561	14.8(16)	15.7(16)	13.2(16)	4.6(13)	0.8(13)	5.4(13)
S7	18.3(6)	22.0(6)	12.3(5)	4.6(5)	6.3(4)	8.4(5)
S8	10.1(5)	13.7(5)	10.3(5)	4.7(4)	2.3(4)	3.0(4)
S9	10.8(5)	10.4(5)	7.9(5)	2.5(4)	1.9(4)	1.9(4)
O71	29(2)	33(2)	30(2)	22.1(19)	18.5(18)	15.1(18)
O72	27(2)	41(3)	14.6(19)	-5.4(17)	5.5(16)	13.0(19)
O73	16.0(17)	14.6(16)	18.6(18)	-0.8(14)	3.4(14)	4.8(13)
O81	17.8(17)	19.9(17)	14.4(17)	9.6(14)	3.4(14)	7.9(14)
O82	11.3(15)	21.8(18)	15.8(17)	6.6(14)	4.6(13)	1.8(13)
O91	16.0(17)	16.2(17)	14.2(17)	3.8(13)	-1.0(13)	1.8(13)
O92	19.3(17)	22.7(18)	16.6(17)	11.2(15)	9.3(14)	9.4(14)
O93	21.8(18)	13.4(16)	10.9(16)	0.2(13)	1.4(13)	7.4(14)
O781	14.6(16)	14.8(16)	13.8(16)	0.6(13)	4.1(13)	3.9(13)
O891	12.1(15)	13.5(15)	8.9(15)	3.9(12)	2.9(12)	2.0(12)
S10	13.1(5)	12.6(5)	19.3(6)	2.1(4)	5.3(4)	3.8(4)
S11	11.3(5)	12.7(5)	14.9(5)	4.9(4)	3.8(4)	2.2(4)
S12	19.3(6)	11.7(5)	12.8(5)	3.4(4)	4.8(4)	1.3(4)
O1	19.2(18)	19.0(18)	23.0(19)	8.1(15)	8.2(15)	2.8(14)
O10B	14.2(16)	13.1(16)	22.2(18)	7.4(14)	5.5(14)	4.8(13)
O11B	14.0(17)	23.1(19)	17.5(18)	8.2(15)	1.3(14)	-2.3(14)
O101	22.8(19)	10.7(16)	27(2)	2.9(14)	11.5(16)	-1.5(14)
O102	17.2(18)	20.4(19)	30(2)	2.7(16)	5.3(16)	10.1(15)
O103	21.8(19)	16.4(17)	20.1(19)	0.6(14)	4.1(15)	9.4(15)
O111	19.4(18)	14.4(17)	27(2)	6.0(15)	9.4(16)	3.6(14)
O112	11.9(16)	23.1(18)	15.8(17)	8.2(14)	2.1(13)	6.5(14)
O122	28(2)	21.7(19)	15.1(18)	5.4(15)	6.7(16)	2.0(16)

O123	38(2)	15.7(18)	22(2)	2.4(15)	13.7(18)	8.2(16)
S13	14.2(5)	17.2(5)	15.2(5)	5.5(4)	8.2(4)	6.4(4)
S14	15.2(5)	14.0(5)	11.3(5)	5.2(4)	6.0(4)	6.7(4)
S15	18.8(6)	11.8(5)	11.7(5)	3.5(4)	-0.4(4)	2.9(4)
O13B	16.2(16)	12.6(15)	13.2(16)	3.7(13)	7.5(13)	3.4(13)
O14B	19.6(17)	12.6(15)	12.4(16)	5.1(13)	3.0(13)	3.8(13)
O131	35(2)	32(2)	34(2)	22.7(19)	23(2)	21.5(19)
O132	30(2)	23(2)	26(2)	-0.9(16)	18.7(18)	4.9(16)
O133	16.1(18)	25(2)	28(2)	-2.0(17)	7.0(16)	4.5(15)
O141	31(2)	17.8(17)	16.8(18)	10.7(14)	12.0(16)	15.4(15)
O142	16.2(17)	23.0(18)	17.7(18)	8.9(15)	10.0(14)	7.3(14)
O151	19.1(19)	19.3(18)	23(2)	6.1(16)	-4.7(15)	-1.0(15)
O152	38(2)	24(2)	16.9(19)	10.2(16)	10.8(17)	13.1(18)
O153	20.9(18)	12.1(16)	20.4(19)	4.3(14)	-0.4(15)	5.2(14)
S16	17.0(5)	12.7(5)	13.9(5)	2.8(4)	7.7(4)	3.6(4)
S17	13.4(5)	10.6(5)	12.6(5)	2.5(4)	3.2(4)	2.3(4)
S18	14.2(6)	15.6(6)	39.8(8)	14.7(6)	-6.1(5)	-1.3(5)
O16B	15.1(16)	14.8(16)	10.1(15)	3.1(12)	4.6(13)	3.6(13)
O17B	12.2(16)	14.4(16)	17.3(17)	5.6(13)	0.6(13)	2.1(13)
O161	27(2)	17.4(18)	25(2)	1.5(15)	13.3(17)	5.4(15)
O162	19.5(18)	16.5(17)	24(2)	3.7(15)	11.2(15)	1.5(14)
O163	20.9(18)	17.0(17)	14.8(17)	2.3(14)	4.1(14)	8.3(14)
O171	14.5(16)	21.7(18)	10.7(16)	3.1(13)	3.9(13)	6.8(14)
O172	21.1(18)	12.2(16)	25(2)	3.8(14)	9.9(16)	2.5(14)
O181	27(3)	13(2)	110(5)	3(3)	-15(3)	5.4(19)
O182	15.2(18)	22(2)	43(3)	15.0(19)	-3.6(18)	0.4(15)
O183	24(2)	58(3)	42(3)	35(3)	0(2)	-11(2)
S19	16.6(5)	20.6(6)	18.4(6)	7.2(5)	10.4(5)	10.4(5)
S20	10.6(5)	13.1(5)	11.8(5)	3.7(4)	4.4(4)	4.2(4)
S21	22.2(6)	14.3(5)	12.2(5)	5.3(4)	6.0(5)	5.2(4)
O19B	18.6(17)	21.6(18)	14.3(16)	7.0(14)	9.1(14)	13.5(14)
O20B	15.8(16)	16.5(16)	10.1(15)	4.9(13)	2.9(13)	3.6(13)
O191	22(2)	32(2)	29(2)	10.0(18)	12.7(17)	17.7(17)

O192	22.9(19)	21.2(19)	26(2)	8.7(16)	13.3(16)	7.7(15)
O193	25.1(19)	18.1(17)	15.6(17)	2.6(14)	5.0(15)	11.6(15)
O201	17.8(17)	15.9(17)	19.6(18)	1.8(14)	7.5(14)	2.7(14)
O202	10.9(15)	18.4(17)	14.3(16)	6.1(13)	4.1(13)	6.0(13)
O211	44(3)	30(2)	17(2)	14.1(17)	6.1(18)	8(2)
O212	35(2)	19(2)	29(2)	-5.4(17)	12.2(19)	5.1(17)
O213	16.8(19)	34(2)	37(2)	17.2(19)	13.3(18)	7.1(17)
S22	16.0(5)	13.2(5)	11.8(5)	3.2(4)	0.2(4)	4.2(4)
S23	11.7(5)	16.9(5)	10.5(5)	1.3(4)	2.7(4)	5.2(4)
S24	13.8(5)	28.1(7)	13.8(6)	2.9(5)	4.3(4)	9.9(5)
O22B	17.3(17)	15.7(16)	11.6(16)	1.2(13)	0.5(13)	2.0(13)
O23B	13.2(16)	15.1(16)	20.0(18)	2.3(14)	5.6(14)	5.3(13)
O23T	15.3(17)	28(2)	16.6(18)	5.7(15)	6.7(14)	5.7(15)
O221	22.0(18)	12.3(16)	14.9(17)	2.4(13)	1.5(14)	3.9(14)
O222	18.9(18)	22.1(19)	22(2)	1.9(15)	2.1(15)	8.9(15)
O223	28(2)	21.5(19)	14.5(18)	9.5(15)	2.1(15)	6.4(16)
O232	18.1(18)	23.6(19)	13.0(17)	-2.2(14)	0.3(14)	5.7(15)
O241	21(3)	16(3)	14(3)	-1(2)	6(2)	5(2)
O242	15(5)	26(6)	15(5)	3(5)	3(4)	4(5)
O243	15(5)	13(5)	23(6)	7(4)	10(5)	10(4)
O244	18(5)	29(6)	25(6)	16(5)	17(5)	11(5)
O245	13(3)	45(4)	27(4)	-12(3)	6(3)	-1(3)
O246	41(4)	48(5)	37(4)	24(4)	19(4)	35(4)

Table S38: Bond Lengths for $[Te_6][HS_3O_{10}]_4$-II in pm.

Atom	Atom	Length/pm	Atom	Atom	Length/pm
Te1	Te2	271.52(5)	S11	O11B	153.3(4)
Te1	Te3	267.78(5)	S11	O111	141.5(4)
Te1	Te4	310.85(5)	S11	O112	141.7(4)
Te2	Te3	269.88(5)	S12	O1	143.0(4)
Te2	Te5	301.34(5)	S12	O11B	175.6(4)
Te3	Te6	321.45(5)	S12	O122	142.1(4)
Te4	Te5	271.56(5)	S12	O123	143.9(4)
Te4	Te6	267.34(5)	S13	O13B	164.4(4)
Te5	Te6	270.15(4)	S13	O131	139.3(4)
Te7	Te8	271.12(5)	S13	O132	142.8(4)
Te7	Te9	270.44(5)	S13	O133	150.8(4)
Te7	Te11	306.65(5)	S14	O13B	160.3(4)
Te8	Te9	268.20(4)	S14	O14B	155.2(4)
Te8	Te10	310.20(5)	S14	O141	141.5(4)
Te9	Te12	319.19(5)	S14	O142	141.4(4)
Te10	Te11	271.45(5)	S15	O14B	171.0(4)
Te10	Te12	267.80(5)	S15	O151	143.3(4)
Te11	Te12	269.17(5)	S15	O152	143.0(4)
S1	O11	142.6(4)	S15	O153	143.6(4)
S1	O12	141.2(4)	S16	O16B	164.7(4)
S1	O13	152.1(4)	S16	O161	140.3(4)
S1	O121	164.0(4)	S16	O162	141.2(4)
S2	O21	141.5(4)	S16	O163	151.3(4)
S2	O22	140.8(4)	S17	O16B	161.3(4)
S2	O121	160.6(4)	S17	O17B	152.7(4)
S2	O231	155.5(3)	S17	O171	141.2(4)
S3	O31	142.3(4)	S17	O172	142.3(4)
S3	O32	142.5(4)	S18	O17B	175.8(4)
S3	O33	143.6(4)	S18	O181	143.2(6)
S3	O231	173.1(4)	S18	O182	141.8(4)
S4	O41	142.4(4)	S18	O183	143.5(6)

S4	O42	140.5(4)	S19	O19B	163.4(4)
S4	O43	151.9(4)	S19	O191	141.7(4)
S4	O451	163.0(4)	S19	O192	142.1(4)
S5	O51	142.0(4)	S19	O193	152.2(4)
S5	O52	141.9(3)	S20	O19B	161.0(4)
S5	O451	161.2(4)	S20	O20B	153.1(4)
S5	O561	153.2(4)	S20	O201	141.8(4)
S6	O61	141.4(4)	S20	O202	142.1(4)
S6	O62	141.5(4)	S21	O20B	177.2(4)
S6	O63	143.2(4)	S21	O211	140.8(4)
S6	O561	177.3(4)	S21	O212	143.4(4)
S7	O71	141.2(4)	S21	O213	142.5(4)
S7	O72	140.7(4)	S22	O22B	170.3(4)
S7	O73	151.4(4)	S22	O221	143.7(4)
S7	O781	163.3(4)	S22	O222	142.9(4)
S8	O81	141.4(4)	S22	O223	143.7(4)
S8	O82	141.4(4)	S23	O22B	156.3(4)
S8	O781	161.2(4)	S23	O23B	159.7(4)
S8	O891	155.4(4)	S23	O23T	140.8(4)
S9	O91	141.9(4)	S23	O232	141.8(4)
S9	O92	142.9(4)	S24	O23B	165.1(4)
S9	O93	144.1(4)	S24	O241	148.5(6)
S9	O891	173.1(3)	S24	O242	139.9(10)
S10	O10B	165.0(4)	S24	O243	143.6(10)
S10	O101	142.1(4)	S24	O244	149.6(10)
S10	O102	141.5(4)	S24	O245	136.3(6)
S10	O103	151.6(4)	S24	O246	145.9(7)
S11	O10B	161.0(4)			

Table S39: Bond Angles for $[Te_6][HS_3O_{10}]_4$-II.

Atom	Atom	Atom	Angle/°	Atom	Atom	Atom	Angle/°
Te2	Te1	Te4	89.522(13)	O103	S10	O10B	103.1(2)
Te3	Te1	Te2	60.050(12)	O11B	S11	O10B	98.3(2)
Te3	Te1	Te4	90.291(13)	O111	S11	O10B	107.8(2)
Te1	Te2	Te5	90.305(13)	O111	S11	O11B	107.9(2)
Te3	Te2	Te1	59.289(12)	O111	S11	O112	119.9(2)
Te3	Te2	Te5	94.167(13)	O112	S11	O10B	107.4(2)
Te1	Te3	Te2	60.661(13)	O112	S11	O11B	113.2(2)
Te1	Te3	Te6	89.462(13)	O1	S12	O11B	104.3(2)
Te2	Te3	Te6	85.865(12)	O1	S12	O123	114.4(3)
Te5	Te4	Te1	88.311(13)	O122	S12	O1	117.7(3)
Te6	Te4	Te1	91.834(13)	O122	S12	O11B	98.5(2)
Te6	Te4	Te5	60.165(12)	O122	S12	O123	116.1(3)
Te4	Te5	Te2	91.538(14)	O123	S12	O11B	102.0(2)
Te6	Te5	Te2	89.953(13)	S11	O10B	S10	120.8(2)
Te6	Te5	Te4	59.144(12)	S11	O11B	S12	126.0(2)
Te4	Te6	Te3	88.127(13)	O131	S13	O13B	108.1(2)
Te4	Te6	Te5	60.692(13)	O131	S13	O132	120.9(3)
Te5	Te6	Te3	89.720(13)	O131	S13	O133	110.6(3)
Te8	Te7	Te11	90.123(13)	O132	S13	O13B	102.2(2)
Te9	Te7	Te8	59.371(12)	O132	S13	O133	111.0(3)
Te9	Te7	Te11	92.794(14)	O133	S13	O13B	102.0(2)
Te7	Te8	Te10	89.896(13)	O14B	S14	O13B	103.1(2)
Te9	Te8	Te7	60.187(13)	O141	S14	O13B	109.0(2)
Te9	Te8	Te10	90.962(13)	O141	S14	O14B	105.5(2)
Te7	Te9	Te12	86.998(13)	O142	S14	O13B	103.9(2)
Te8	Te9	Te7	60.442(13)	O142	S14	O14B	112.1(2)
Te8	Te9	Te12	88.918(12)	O142	S14	O141	121.7(2)
Te11	Te10	Te8	89.313(13)	O151	S15	O14B	99.4(2)
Te12	Te10	Te8	90.911(13)	O151	S15	O153	115.9(3)
Te12	Te10	Te11	59.884(12)	O152	S15	O14B	104.7(2)
Te10	Te11	Te7	90.588(13)	O152	S15	O151	116.2(3)

Te12	Te11	Te7	89.824(13)	O152	S15	O153	115.2(3)
Te12	Te11	Te10	59.383(12)	O153	S15	O14B	102.0(2)
Te10	Te12	Te9	89.113(13)	S14	O13B	S13	124.5(2)
Te10	Te12	Te11	60.732(12)	S14	O14B	S15	123.5(2)
Te11	Te12	Te9	90.305(13)	O161	S16	O16B	102.1(2)
O11	S1	O13	111.4(2)	O161	S16	O162	122.1(2)
O11	S1	O121	107.2(2)	O161	S16	O163	109.1(2)
O12	S1	O11	121.9(2)	O162	S16	O16B	107.2(2)
O12	S1	O13	109.3(2)	O162	S16	O163	110.9(2)
O12	S1	O121	102.3(2)	O163	S16	O16B	103.5(2)
O13	S1	O121	102.5(2)	O17B	S17	O16B	99.2(2)
O21	S2	O121	109.8(2)	O171	S17	O16B	107.7(2)
O21	S2	O231	105.4(2)	O171	S17	O17B	113.1(2)
O22	S2	O21	121.8(2)	O171	S17	O172	120.0(2)
O22	S2	O121	102.9(2)	O172	S17	O16B	107.9(2)
O22	S2	O231	112.6(2)	O172	S17	O17B	106.9(2)
O231	S2	O121	102.76(19)	O181	S18	O17B	100.4(3)
O31	S3	O32	116.3(2)	O181	S18	O183	117.2(4)
O31	S3	O33	116.7(2)	O182	S18	O17B	97.8(2)
O31	S3	O231	104.0(2)	O182	S18	O181	116.6(3)
O32	S3	O33	115.4(2)	O182	S18	O183	116.3(3)
O32	S3	O231	98.33(19)	O183	S18	O17B	103.4(2)
O33	S3	O231	101.9(2)	S17	O16B	S16	120.7(2)
S2	O121	S1	126.0(2)	S17	O17B	S18	124.7(2)
S2	O231	S3	124.1(2)	O191	S19	O19B	101.5(2)
O41	S4	O43	111.7(2)	O191	S19	O192	122.0(3)
O41	S4	O451	107.2(2)	O191	S19	O193	109.0(2)
O42	S4	O41	122.6(2)	O192	S19	O19B	107.1(2)
O42	S4	O43	108.1(3)	O192	S19	O193	111.7(2)
O42	S4	O451	102.0(2)	O193	S19	O19B	103.5(2)
O43	S4	O451	103.0(2)	O20B	S20	O19B	98.1(2)
O51	S5	O451	108.4(2)	O201	S20	O19B	107.9(2)
O51	S5	O561	108.5(2)	O201	S20	O20B	108.4(2)

O52	S5	O51	119.5(2)	O201	S20	O202	119.9(2)
O52	S5	O451	107.3(2)	O202	S20	O19B	107.1(2)
O52	S5	O561	112.9(2)	O202	S20	O20B	113.1(2)
O561	S5	O451	98.0(2)	O211	S21	O20B	97.3(2)
O61	S6	O62	117.0(3)	O211	S21	O212	116.0(3)
O61	S6	O63	116.3(3)	O211	S21	O213	117.6(3)
O61	S6	O561	97.7(2)	O212	S21	O20B	100.9(2)
O62	S6	O63	116.7(3)	O213	S21	O20B	103.5(2)
O62	S6	O561	103.2(2)	O213	S21	O212	116.5(3)
O63	S6	O561	101.0(2)	S20	O19B	S19	120.4(2)
S5	O451	S4	120.5(2)	S20	O20B	S21	123.3(2)
S5	O561	S6	122.6(2)	O221	S22	O22B	102.8(2)
O71	S7	O73	108.6(3)	O222	S22	O22B	104.4(2)
O71	S7	O781	108.2(2)	O222	S22	O221	115.6(2)
O72	S7	O71	121.3(3)	O222	S22	O223	116.0(3)
O72	S7	O73	111.7(2)	O223	S22	O22B	98.5(2)
O72	S7	O781	102.7(2)	O223	S22	O221	115.9(2)
O73	S7	O781	102.6(2)	O22B	S23	O23B	103.4(2)
O81	S8	O82	121.5(2)	O23T	S23	O22B	112.4(2)
O81	S8	O781	109.5(2)	O23T	S23	O23B	104.1(2)
O81	S8	O891	106.4(2)	O23T	S23	O232	122.1(2)
O82	S8	O781	102.8(2)	O232	S23	O22B	104.8(2)
O82	S8	O891	112.6(2)	O232	S23	O23B	108.6(2)
O891	S8	O781	102.46(19)	O241	S24	O23B	100.1(3)
O91	S9	O92	116.6(2)	O242	S24	O23B	105.8(5)
O91	S9	O93	116.1(2)	O242	S24	O243	113.4(8)
O91	S9	O891	98.3(2)	O242	S24	O244	114.7(8)
O92	S9	O93	115.5(2)	O243	S24	O23B	102.9(5)
O92	S9	O891	103.9(2)	O243	S24	O244	111.4(7)
O93	S9	O891	102.50(19)	O244	S24	O23B	107.5(4)
S8	O781	S7	125.5(2)	O245	S24	O23B	109.5(3)
S8	O891	S9	124.4(2)	O245	S24	O241	112.7(5)
O101	S10	O10B	106.7(2)	O245	S24	O246	121.6(5)

O101	S10	O103	111.5(2)	O246	S24	O23B	99.9(3)
O102	S10	O10B	102.3(2)	O246	S24	O241	110.1(4)
O102	S10	O101	122.0(3)	S23	O22B	S22	122.8(2)
O102	S10	O103	109.1(2)	S23	O23B	S24	123.7(2)

Table S40: Torsion Angles for $[Te_6][HS_3O_{10}]_4$-II.

A	B	C	D	Angle/°	A	B	C	D	Angle/°
O11	S1	O121	S2	-35.9(3)	O131	S13	O13B	S14	40.2(4)
O12	S1	O121	S2	-165.3(3)	O132	S13	O13B	S14	168.7(3)
O13	S1	O121	S2	81.5(3)	O133	S13	O13B	S14	-76.4(3)
O21	S2	O121	S1	45.9(3)	O141	S14	O13B	S13	-47.3(3)
O21	S2	O231	S3	165.0(3)	O141	S14	O14B	S15	-166.2(3)
O22	S2	O121	S1	177.0(3)	O142	S14	O13B	S13	-178.3(3)
O22	S2	O231	S3	30.1(3)	O142	S14	O14B	S15	-31.6(4)
O31	S3	O231	S2	-52.8(3)	O151	S15	O14B	S14	-163.2(3)
O32	S3	O231	S2	-172.7(3)	O152	S15	O14B	S14	76.5(3)
O33	S3	O231	S2	69.0(3)	O153	S15	O14B	S14	-44.0(3)
O121	S2	O231	S3	-80.0(3)	O16B	S17	O17B	S18	86.6(3)
O231	S2	O121	S1	-65.9(3)	O17B	S17	O16B	S16	175.3(2)
O41	S4	O451	S5	43.9(3)	O161	S16	O16B	S17	-176.7(3)
O42	S4	O451	S5	173.9(3)	O162	S16	O16B	S17	-47.3(3)
O43	S4	O451	S5	-74.0(3)	O163	S16	O16B	S17	70.0(3)
O51	S5	O451	S4	-75.6(3)	O171	S17	O16B	S16	-66.7(3)
O51	S5	O561	S6	170.2(3)	O171	S17	O17B	S18	-27.2(4)
O52	S5	O451	S4	54.7(3)	O172	S17	O16B	S16	64.2(3)
O52	S5	O561	S6	35.4(3)	O172	S17	O17B	S18	-161.4(3)
O61	S6	O561	S5	175.5(3)	O181	S18	O17B	S17	-66.4(4)
O62	S6	O561	S5	-64.3(3)	O182	S18	O17B	S17	174.6(3)
O63	S6	O561	S5	56.7(3)	O183	S18	O17B	S17	55.1(4)
O451	S5	O561	S6	-77.3(3)	O19B	S20	O20B	S21	82.5(3)
O561	S5	O451	S4	171.8(3)	O20B	S20	O19B	S19	-171.9(3)
O71	S7	O781	S8	-35.5(4)	O191	S19	O19B	S20	-172.2(3)
O72	S7	O781	S8	-164.8(3)	O192	S19	O19B	S20	-43.3(3)

O73	S7	O781	S8	79.1(3)	O193	S19	O19B	S20	74.8(3)
O81	S8	O781	S7	52.4(3)	O201	S20	O19B	S19	75.6(3)
O81	S8	O891	S9	160.6(3)	O201	S20	O20B	S21	-165.5(3)
O82	S8	O781	S7	-177.2(3)	O202	S20	O19B	S19	-54.7(3)
O82	S8	O891	S9	25.3(3)	O202	S20	O20B	S21	-30.1(3)
O91	S9	O891	S8	-177.1(3)	O211	S21	O20B	S20	-176.6(3)
O92	S9	O891	S8	-56.9(3)	O212	S21	O20B	S20	-58.3(3)
O93	S9	O891	S8	63.8(3)	O213	S21	O20B	S20	62.7(3)
O781	S8	O891	S9	-84.5(3)	O22B	S23	O23B	S24	60.4(3)
O891	S8	O781	S7	-60.2(3)	O23B	S23	O22B	S22	79.3(3)
O1	S12	O11B	S11	44.6(4)	O23T	S23	O22B	S22	-32.3(4)
O10B	S11	O11B	S12	108.9(3)	O23T	S23	O23B	S24	178.0(3)
O11B	S11	O10B	S10	173.9(3)	O221	S22	O22B	S23	-41.7(3)
O101	S10	O10B	S11	-48.2(3)	O222	S22	O22B	S23	79.4(3)
O102	S10	O10B	S11	-177.4(3)	O223	S22	O22B	S23	-160.9(3)
O103	S10	O10B	S11	69.4(3)	O232	S23	O22B	S22	-166.9(3)
O111	S11	O10B	S10	62.0(3)	O232	S23	O23B	S24	-50.6(3)
O111	S11	O11B	S12	-139.2(3)	O241	S24	O23B	S23	-84.0(4)
O112	S11	O10B	S10	-68.5(3)	O242	S24	O23B	S23	77.2(7)
O112	S11	O11B	S12	-4.1(4)	O243	S24	O23B	S23	-163.5(6)
O122	S12	O11B	S11	166.1(3)	O244	S24	O23B	S23	-45.8(6)
O123	S12	O11B	S11	-74.8(4)	O245	S24	O23B	S23	34.5(5)
O13B	S14	O14B	S15	79.5(3)	O246	S24	O23B	S23	163.3(4)
O14B	S14	O13B	S13	64.5(3)					

Table S41: Hydrogen Atom Coordinates (Å×10^4) and Isotropic Displacement Parameters (Å^2×10^3) for $[Te_6][HS_3O_{10}]_4$-II.

Atom	*x*	*y*	*z*	U(eq)
H13	5166.81	5682.54	4532.78	28
H43	8078.14	6535.63	5713.5	30
H73	11269.36	9037.56	7061.78	26
H103	3639.4	1700.67	6306.74	30
H133	3243.75	-486.37	7731.55	37
H163	6784.7	3282.36	9135.97	27
H193	8702.21	1613.02	11322.82	29
H241	9681.81	4105.3	261.57	27
H244	9659.27	5361.79	750.67	30

Table S42: Atomic Occupancy for $[Te_6][HS_3O_{10}]_4$-II.

Atom	Occupancy	Atom	Occupancy	Atom	Occupancy
O241	0.6666	H241	0.6666	O242	0.3333
O243	0.3333	O244	0.3333	H244	0.3333
O245	0.6666	O246	0.6666		

$[Te_6][S_4O_{13}]_2$ (7)

Table S43: Crystallographic data of $[Te_6][S_4O_{13}]_2$.

Empirical formula	$O_{13}S_4Te_3$
Formula weight	719.04 g/mol
Temperature	100.00 K
Crystal system	orthorhombic
Space group	Pnma (No. 62)
Unit cell dimensions	a = 1450.91(8) pm
	b = 1909.90(10) pm
	c = 946.18(5) pm
	α = 90°
	β = 90°
	γ = 90°
Volume	2622.0(2) Å^3
Z	8
ρ_{calc}	3.643 g/cm^3
μ	7.322 mm^{-1}
F(000)	2592
Crystal size	0.04 × 0.03 × 0.02 mm^3
Radiation	MoK_α (λ = 0.71073 nm)
2Θ range for data collection	4.266 to 57.4
Index ranges	-19 ≤ h ≤ 19, -25 ≤ k ≤ 25, -12 ≤ l ≤ 12
Reflections collected	72748
Independent reflections	3490 [R_{int} = 0.0884, R_σ = 0.0272]
Completeness	100%
Absorption correction	Multiscan
Min. and max. transmission	0.633 / 0.747
Data/restraints/parameters	72748/0/184
Goodness-of-fit on F^2	1.098
Final R indexes [I≥2σ (I)]	R_1 = 0.0339, wR_2 = 0.0616
Final R indexes [all data]	R_1 = 0.0503, wR_2 = 0.0680
Largest diff. peak/hole	1.02/–0.99 e · Å^{-3}

CCDC-No.	2502407

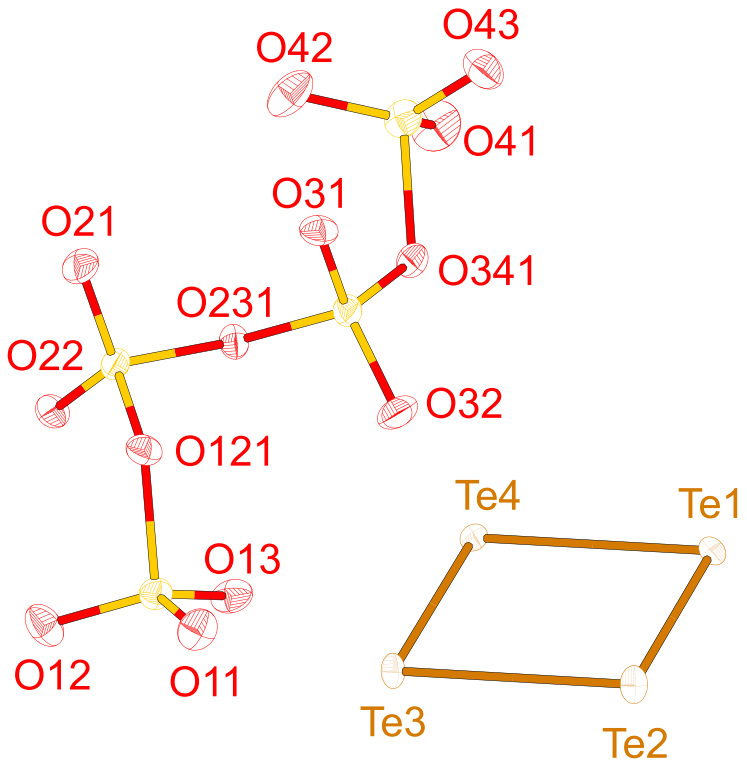

Figure S21: Thermal ellipsoid plot of the asymmetric unit of $[Te_6][S_4O_{13}]_2$ shown with 50% probability.

Table S44: Fractional Atomic Coordinates ($\times 10^4$) and Equivalent Isotropic Displacement Parameters ($Å^2 \times 10^3$) for $[Te_6][S_4O_{13}]_2$. U_{eq} is defined as 1/3 of the trace of the orthogonalised U_{IJ} tensor.

Atom	*x*	*y*	*z*	U(eq)
Te1	7604.1(3)	3206.0(2)	-64.1(4)	13.10(9)
Te2	6912.9(4)	2500	2182.1(6)	14.62(12)
Te3	4949.6(4)	2500	767.9(6)	13.49(12)
Te4	5660.4(3)	3204.0(2)	-1472.0(4)	12.81(9)
S1	2816.5(11)	3498.1(8)	8956.0(16)	16.0(3)
S2	2499.3(11)	4879.6(8)	7803.4(16)	15.0(3)
S3	4415.2(10)	5227.5(8)	7953.6(17)	15.9(3)
S4	4911.3(12)	6319.6(9)	5994.0(17)	20.0(3)
O11	3133(3)	3358(3)	10352(5)	22.5(10)
O12	1903(3)	3277(3)	8614(5)	23.7(10)
O13	3468(3)	3412(2)	7832(5)	21.2(10)
O21	2197(3)	5532(2)	8316(5)	21.8(10)
O22	2002(3)	4515(2)	6737(5)	18.0(9)

O31	4157(3)	5790(2)	8850(5)	17.8(9)
O32	4820(3)	4618(2)	8531(5)	23.8(10)
O41	5211(4)	6187(3)	4589(5)	30.7(12)
O42	3970(4)	6492(3)	6216(5)	28.7(12)
O43	5554(3)	6688(3)	6876(5)	26.3(11)
O121	2712(3)	4416(2)	9096(5)	17.4(9)
O231	3495(3)	4977(2)	7084(5)	15.9(9)
O341	4976(3)	5465(2)	6674(5)	20.1(10)

Table S45: Anisotropic Displacement Parameters ($Å^2 \times 10^3$) for $[Te_6][S_4O_{13}]_2$. The anisotropic displacement factor exponent takes the form: $-2\pi^2[h^2a^{*2}U_{11}+2hka^*b^*U_{12}+\ldots]$.

Atom	U_{11}	U_{22}	U_{33}	U_{23}	U_{13}	U_{12}
Te1	11.20(17)	12.02(17)	16.07(18)	0.46(15)	-0.41(14)	-2.79(15)
Te2	11.4(3)	22.2(3)	10.3(3)	0	-0.1(2)	0
Te3	8.5(2)	19.2(3)	12.8(3)	0	1.7(2)	0
Te4	11.70(17)	11.72(17)	15.02(18)	2.53(15)	-1.12(14)	1.22(14)
S1	16.9(7)	16.1(7)	15.0(7)	2.2(6)	-0.2(6)	0.5(6)
S2	13.0(7)	13.9(7)	18.1(7)	-2.8(6)	-2.9(6)	2.0(6)
S3	12.8(7)	14.7(7)	20.2(7)	-3.8(6)	-1.4(6)	0.0(6)
S4	21.2(8)	21.9(8)	16.8(8)	-0.3(6)	5.9(6)	3.1(7)
O11	24(2)	27(3)	16(2)	3.3(19)	-1.3(19)	3(2)
O12	23(2)	28(3)	20(2)	4(2)	-5(2)	-9(2)
O13	26(2)	17(2)	20(2)	-1.1(19)	8(2)	4.8(19)
O21	20(2)	17(2)	28(3)	-7.2(19)	0(2)	4.2(19)
O22	18(2)	16(2)	20(2)	-3.9(18)	-5.2(18)	-3.0(18)
O31	23(2)	13(2)	18(2)	-3.2(17)	-2.6(18)	-1.4(18)
O32	25(3)	16(2)	31(3)	-3(2)	-7(2)	7(2)
O41	37(3)	38(3)	18(2)	-4(2)	9(2)	5(2)
O42	31(3)	34(3)	22(3)	4(2)	6(2)	15(2)
O43	24(3)	22(3)	32(3)	-8(2)	9(2)	-6(2)
O121	20(2)	14(2)	19(2)	-1.5(17)	-1.3(18)	-2.6(17)
O231	13(2)	18(2)	17(2)	-2.7(18)	0.8(17)	-0.7(17)
O341	15(2)	17(2)	28(2)	-4.0(19)	4.1(19)	3.4(18)

Table S46: Bond Lengths for $[Te_6][S_4O_{13}]_2$ in pm.

Atom	Atom	Length/pm	Atom	Atom	Length/pm
Te1	Te1[1]	269.67(8)	S2	O22	142.3(4)
Te1	Te2	270.93(6)	S2	O121	154.1(5)
Te1	Te4	311.90(6)	S2	O231	160.9(5)
Te2	Te3	314.71(8)	S3	O31	141.9(5)
Te3	Te4[1]	271.35(6)	S3	O32	141.3(5)
Te3	Te4	271.35(6)	S3	O231	163.9(5)
Te4	Te4[1]	268.91(8)	S3	O341	152.7(5)
S1	O11	142.4(5)	S4	O41	142.1(5)
S1	O12	142.8(5)	S4	O42	142.1(5)
S1	O13	143.2(5)	S4	O43	143.5(5)
S1	O121	176.4(5)	S4	O341	175.6(5)
S2	O21	140.7(5)			

[1] +X, ½-Y, +Z

Table S47: Bond Angles for $[Te_6][S_4O_{13}]_2$.

Atom	Atom	Atom	Angle/°	Atom	Atom	Atom	Angle/°
Te1[1]	Te1	Te2	60.154(11)	O21	S2	O231	108.9(3)
Te1[1]	Te1	Te4	89.930(11)	O22	S2	O121	112.5(3)
Te2	Te1	Te4	89.985(18)	O22	S2	O231	102.2(3)
Te1[1]	Te2	Te1	59.69(2)	O121	S2	O231	102.9(2)
Te1	Te2	Te3	90.087(19)	O31	S3	O231	107.8(3)
Te1[1]	Te2	Te3	90.087(19)	O31	S3	O341	112.9(3)
Te4[1]	Te3	Te2	89.317(19)	O32	S3	O31	120.1(3)
Te4	Te3	Te2	89.318(19)	O32	S3	O231	107.0(3)
Te4[1]	Te3	Te4	59.41(2)	O32	S3	O341	109.3(3)
Te3	Te4	Te1	90.609(18)	O341	S3	O231	97.0(2)
Te4[1]	Te4	Te1	90.069(11)	O41	S4	O42	118.3(3)
Te4[1]	Te4	Te3	60.297(10)	O41	S4	O43	115.6(3)
O11	S1	O12	117.0(3)	O41	S4	O341	99.3(3)
O11	S1	O13	117.0(3)	O42	S4	O43	115.1(3)
O11	S1	O121	98.3(3)	O42	S4	O341	102.3(3)
O12	S1	O13	114.2(3)	O43	S4	O341	102.0(3)

O12	S1	O121	103.4(3)	S2	O121	S1	121.9(3)
O13	S1	O121	103.1(3)	S2	O231	S3	123.6(3)
O21	S2	O22	121.3(3)	S3	O341	S4	122.6(3)
O21	S2	O121	107.3(3)				

[1] +X, ½-Y, +Z

Table S48: Torsion Angles for $[Te_6][S_4O_{13}]_2$.

A	B	C	D	Angle/°	A	B	C	D	Angle/°
O11	S1	O121	S2	172.2(3)	O32	S3	O231	S2	86.6(4)
O12	S1	O121	S2	-67.4(4)	O32	S3	O341	S4	-160.7(3)
O13	S1	O121	S2	51.9(4)	O41	S4	O341	S3	-156.8(4)
O21	S2	O121	S1	163.0(3)	O42	S4	O341	S3	-35.0(4)
O21	S2	O231	S3	63.1(4)	O43	S4	O341	S3	84.4(4)
O22	S2	O121	S1	27.0(4)	O121	S2	O231	S3	-50.5(4)
O22	S2	O231	S3	-167.3(3)	O231	S2	O121	S1	-82.3(3)
O31	S3	O231	S2	-43.9(4)	O231	S3	O341	S4	88.5(3)
O31	S3	O341	S4	-24.3(4)	O341	S3	O231	S2	-160.7(3)

Table S 49: S–O bond lengths (in pm) and δ-values (terminal SO_3) groups of literature-known tetrasulfate compounds. [TS] = $[S_4O_{13}]^{2-}$.

Bond	$[Te_6]$ $[TS]_2$	$[IBr_2]_2$ $[TS]$[16]	$[I_3]_4$ $[TS]_2(SO_3)$[16]	Ba $[TS]$[b] [17]	$[NO_2]_2$ $[TS]$[a] [18]	Li_2 $[TS]$ [12]
S1–O11	142.4(5)	144.2(3)	142.8(9)–144(1)	142.6(8)	142.0	143.1(2)
S1–O12	142.8(5)	143.3(3)	143(1)–144.3(9)	142.7(8)	142.3	142.5(2)
S1–O13	143.2(5)	142.6(3)	143(1)–145(1)	142.6(8)	142.3	142.4(2)
δ(S1)	*10.33*	*10.96*	*10.52*	*9.20*	*9.80*	*9.57*
S1–O121	176.4(5)	171.3(3)	171.2(9)–174.0(9)	178.7(8)	176.6	176.5(2)
S2–O21	140.7(5)	141.0(3)	140(1)–141.2(9)	141.9(8)	141.4	140.9(2)
S2–O22	142.3(4)	141.2(3)	141(1)–141(1)	142.0(8)	141.1	141.0(2)
S2–O121	154.1(5)	156.3(3)	155.6(9)–155.7(9)	152.4(8)	153.0	152.4(2)
S2–O231	160.9(5)	161.6(3)	162(1)–163.3(9)	161.8(5)	163.9	162.8(2)
S3–O31	141.9(5)	140.0(3)	141(1)–141.5(9)	141.9(8)	141.3	141.7(2)
S3–O32	141.3(5)	140.4(3)	140(1)–144(1)	142.0(8)	142.0	140.9(2)
S3–O231	163.9(5)	163.2(3)	161.3(9)–162.8(9)	161.8(5)	160.9	161.7(2)
S3–O341	152.7(5)	155.6(3)	155.5(9)–156.7(9)	152.4(8)	153.4	153.2(2)
S4–O41	142.1(5)	143.7(3)	142.4(9)–143.9(8)	142.6(8)	142.1	142.1(2)
S4–O42	142.1(5)	142.5(3)	142.9(9)–146(1)	142.7(8)	143.1	141.8(2)
S4–O43	143.5(5)	144.2(3)	142.4(9)–144.0(8)	142.6(8)	143.1	142.1(2)
δ(S4)	*9.87*	*10.92*	*10.50*	*9.20*	*9.52*	*9.85*
S4–O341	175.6(5)	170.5(3)	172.3(9)–174.7(8)	178.7(8)	177.0	175.3(2)

a – the average lengths were calculated, b – symmetry plane through the anion leads to S3 = S2 and S4 = S1.

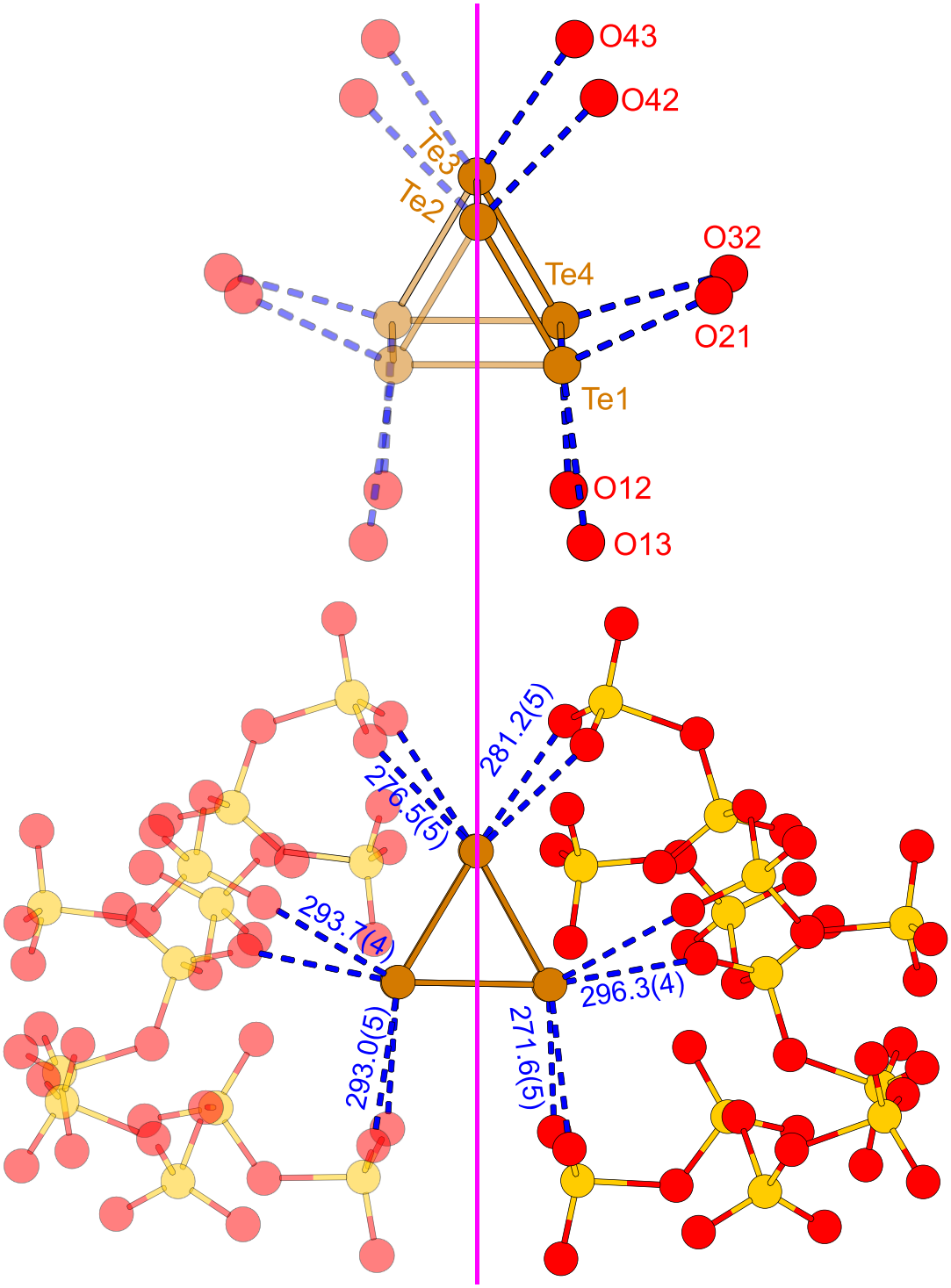

Figure S 22: Chalcogen-bonding (D–A distance below 300 pm) within $[Te_6][S_4O_{13}]_2$. Distances are given in pm. O–Te coordination within the two $[Te_6]$ plane is shown at the top. The atoms that are generated via the mirror plane are shown at 50% visibility. The mirror plane is indicated by the vertical magenta line.

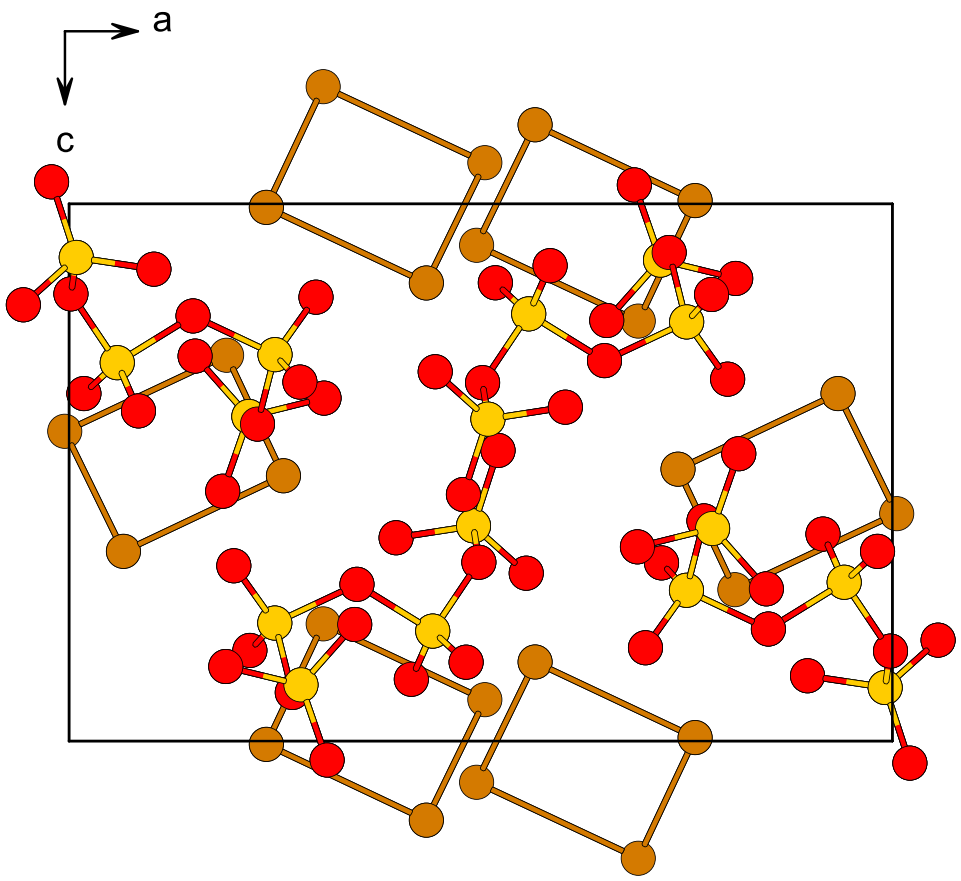

Figure S 23: Packed unit cell of $[Te_6][S_4O_{13}]_2$ viewed along the crystallographic b-axis.

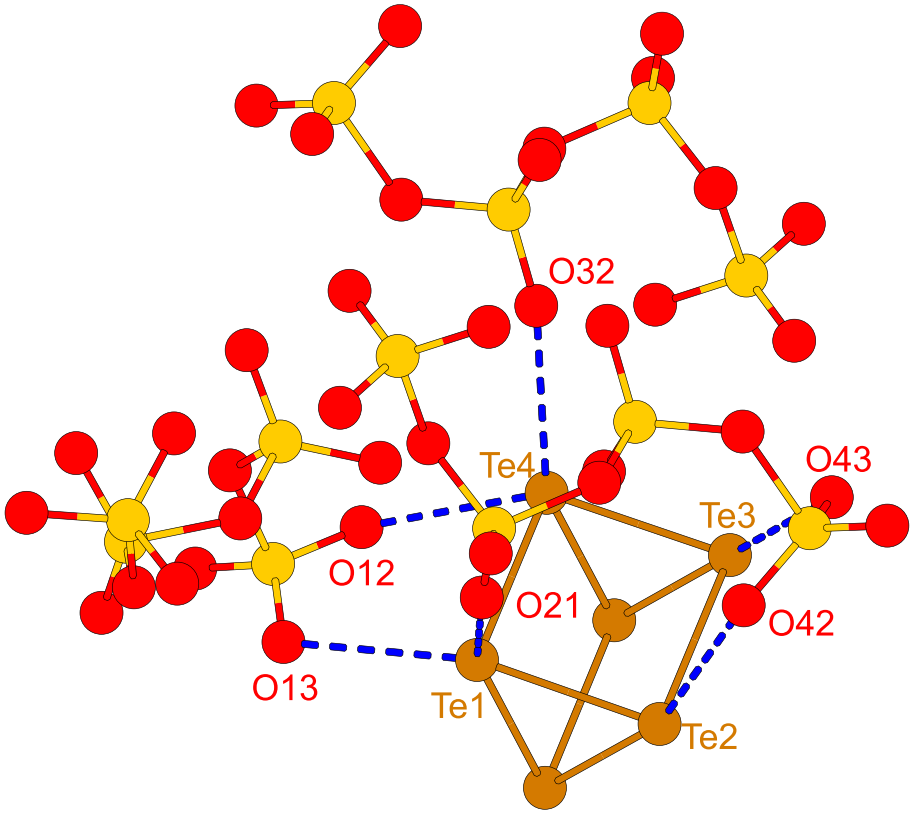

Figure S 24: Mono- and bidentate coordination of coordinating oxygen atoms and auxiliary coordination of terminal oxygen atoms within the polysulfate chain (O32) within $[Te_6][S_4O_{13}]_2$.

D. Delta Values

The delta values (in the following written as δ) were calculated using the Polynator software package.[19] We have described this process in more detail before.[16] Within the software, the central and ligand atoms were defined as sulfur and oxygen, respectively. The terminal SO_3 units could be identified in most cases by adjusting the distance connectivity criterium to a maximum value of 1.6 Å. For the analysis, the generated δ values for the geometric object 'triangle[regular] (–6m2, 1 °f)' were taken.

Table S 50: Relevant bond lengths and δ values for the novel compounds.

LB-S bond length [pm]	Delta (triangle) [δ]	CCDC/CSD	Compound / Reference	Legend
166	12,198	2477856	$[Se_4][HS_2O_7]_2$ [*this work*]	$[Se_4][HS_2O_7]_2$
164,69	12.143	2504489	$[Se_4][S_2O_7]$ [*this work*]	$[Se_4][S_2O_7]$
164,77	12,12	2405909	$[ICl_2][HS_2O_7]$[16]	$[ICl_2][HS_2O_7]$
164,08	12.103	2504489	$[Se_4][S_2O_7]$ [*this work*]	$[Se_4][S_2O_7]$
165,1	11,965	26138	$Pd[HS_2O_7]_2$[20]	$Pd[HS_2O_7]_2$
168,3	11,738	428615	$[NO][HS_2O_7]$[21]	$[NO][HS_2O_7]$
167,77	11,735	428573	$Rb[HS_3O_{10}]$[22]	$Rb[HS_3O_{10}]$
167,96	11,734	428796	$[NH_4][HS_2O_7]$[21]	$[NH_4][HS_2O_7]$
169,08	11,728	428570	$K[HS_3O_{10}]$[22]	$K[HS_3O_{10}]$
166,69	11,693	428724	$Cs[HS_2O_7]$[21]	$Cs[HS_2O_7]$

168,5	11,637	428564	$K[HS_2O_7]$[21]	$K[HS_2O_7]$
168,89	11,562	429114	$Rb[HS_2O_7]$[21]	$Rb[HS_2O_7]$
170,06	10,937	428571	$Na[HS_3O_{10}]$[22]	$Na[HS_3O_{10}]$
171,4	10,912	2476929	$[Te_6][HS_3O_{10}]_4$ *[this work]*	$[Te_6][HS_3O_{10}]_4$
171	10,569	2476927	$[Se_4][HS_3O_{10}]_2$ *[this work]*	$[Se_4][HS_3O_{10}]_2$
174,4	10,515	2476929	$[Te_6][HS_3O_{10}]_4$ *[this work]*	$[Te_6][HS_3O_{10}]_4$
170,9	10,488	2476926	$[Te_4][HS_3O_{10}]_2$ *[this work]*	$[Te_4][HS_3O_{10}]_2$
172,6	10,471	2476929	$[Te_6][HS_3O_{10}]_4$ *[this work]*	$[Te_6][HS_3O_{10}]_4$
176,4	10,325	2502407	$[Te_6][S_4O_{13}]_2$ *[this work]*	$[Te_6][S_4O_{13}]_2$
175,1	10,069	2476929	$[Te_6][HS_3O_{10}]_4$ *[this work]*	$[Te_6][HS_3O_{10}]_4$
175,6	9,867	2502407	$[Te_6][S_4O_{13}]_2$ *[this work]*	$[Te_6][S_4O_{13}]_2$

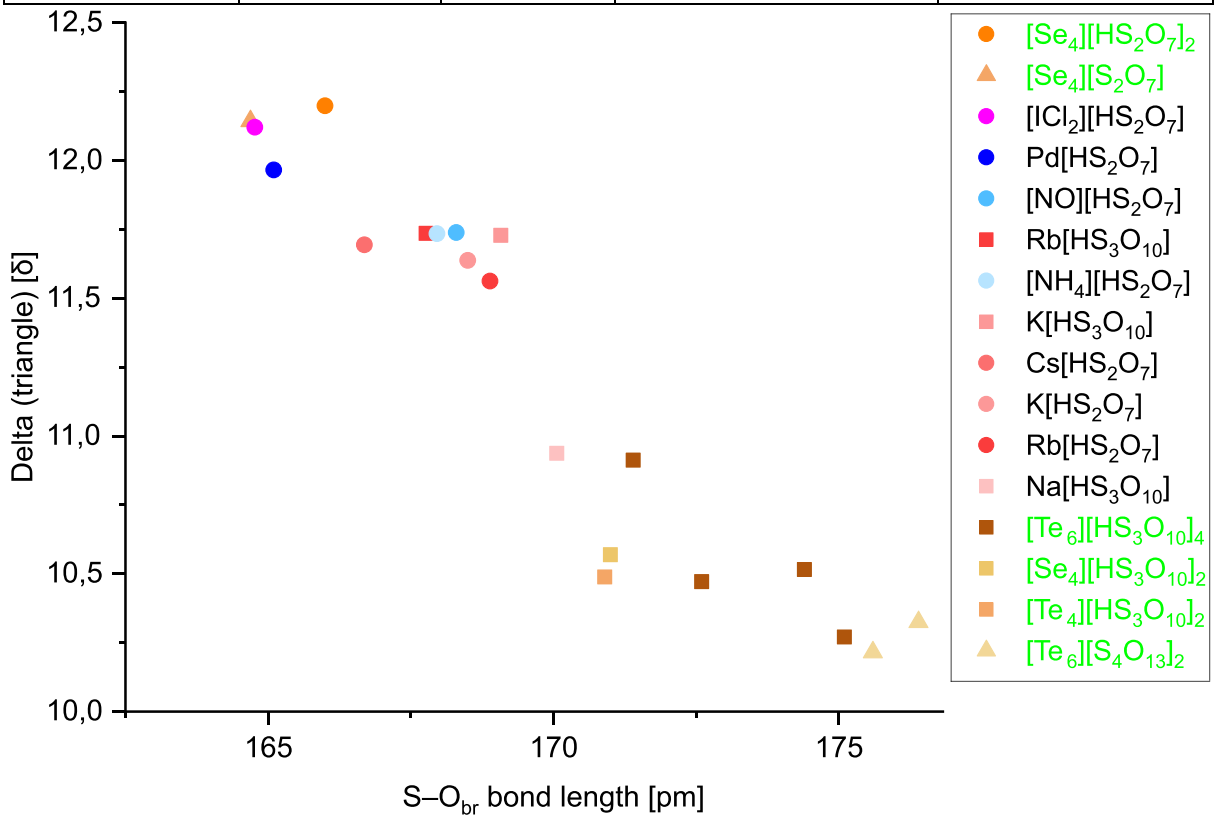

Figure S 25: δ values for the different SO_3 units within the novel compound as a function of the respective donor-acceptor distance (i.e. the S–O–S bridging bond length).

E. Spectroscopic investigations

All spectra were recorded with an inVia Qotor confocal Raman microscope, equipped with 10x, 50x and 100x magnification lenses, from Renishaw GmbH (Pliezhausen, GER). The spectra were measured on selected single crystals samples at room temperature using a green laser (λ= 532 nm, 100 mW) and varying exposure times. The data was processed with the WiRE 5.1 software.[23] The data was plotted using the software OriginPro.[24]

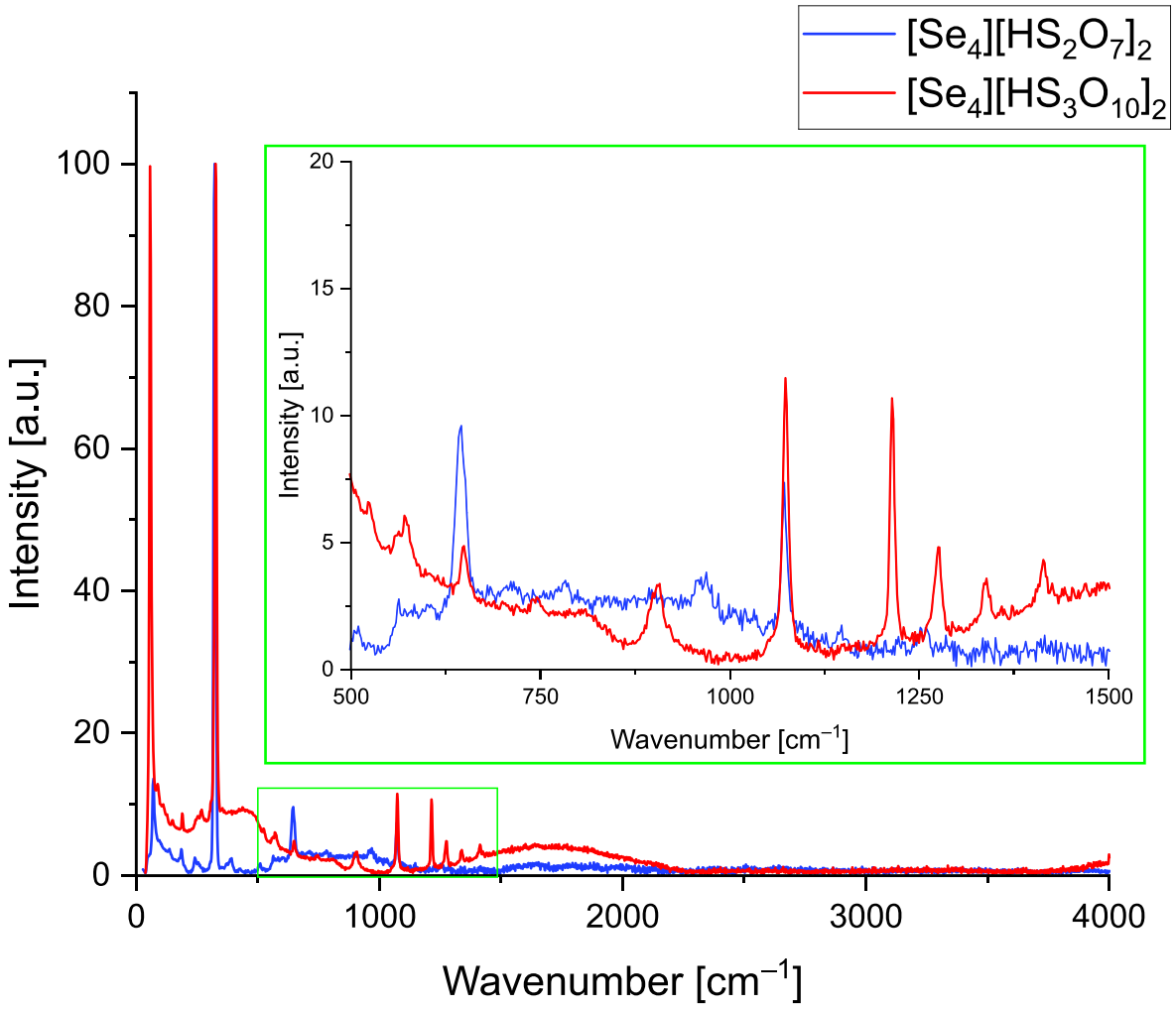

Figure S 26: Raman spectra of compounds **1** (blue) and **2** (red). The raw data was normalized [0,100] using the software Origin.

Table S51*:* Raman frequencies (in cm^{-1}) of compounds **1** and **2** compared to reference compounds and previously reported values.

$[Se_4][HS_2O_7]_2$[25]	$[Se_4][HS_2O_7]_2$ (*this work*)	$[Se_4][HS_3O_{10}]_2$ (*this work*)	Assignment
		1415	
		1338	
		1274	ν_{as} S–O[26]
		1213	
	1071	1071	ν_s S–O[27]
		907	
	645	649	δ_{as} S–O [19]
	509	524	δ_s S–O [19]
487			S–OH (def.)[28]
393	392	392	
324	322	326	
307			$[Se_4]^{2+}$ fundamentals [25, 29]
296		269	
260	240	253	
191	185	188	
		86	
73	71	71	Lattice modes
58		57	
46			

as = asymmetric, s = symmetric, def. = deformation.

F. Computational Details

All calculations were computed using the TURBOMOLE 7.7 software package, [30] except for the NBO calculations which were obtained using the NBO 7.0[31] extension of the Gaussian16[32] software. The geometries of the calculated assemblies were taken from the crystal X-ray structures. The PBE0 hybrid functional[33] with the D4 dispersion correction[34] was employed, in conjunction with the def2-TZVP basis set.[35-36]

The quantum theory of atoms in molecules (QTAIM) analysis[37], NCIplots[38] and the molecular electrostatic potential (MEP) cubes were obtained through the Multiwfn[39] program, using the wavefunction file obtained from the calculations. The topological parameters, including bond critical points (bcps) and electron density values, were extracted to characterize chalcogen bonding interactions.

The chalcogen bond interaction energies were obtained through an energy descriptor based on the potential energy density (V) found in a bond critical point interconnecting the chalcogen atom with the Lewis base.[40] For Se, the interaction energy was computed as: E_{int} = 0.375 V(ρ); and for Te, the interaction energy was computed as: E_{int} = 0.556 V(ρ).

Results and Discussion

We analyzed the supramolecular assemblies by characterizing the Ch···O chalcogen bonds (ChB) using the Quantum Theory of Atoms-In-Molecules (QTAIM) and the Non-Covalent Interaction (NCI) plot analysis (see Figure S 27). All identified Ch···O contacts are characterized by the presence of a bond critical point (BCPs, shown as a small red sphere) and a bond path (orange line) interconnecting the Ch (Se, Te) and O atoms. The NCI plot results, represented by the reduced density gradient (RDG) isosurfaces, are observed coincident with the BCP locations, with the color ranging from green to blue, indicating weak to moderate attractive interactions. Inspection of the QTAIM/NCIplot results reveals the existence of three primary binding modes: bifurcated Ch···O,O ChBs, bifurcated Ch,Ch···O ChBs, and standard Ch···O ChBs where only one donor and one acceptor atom are involved. The strength of each ChB was estimated using an energy predictor based on the QTAIM potential energy density (V), allowing for the evaluation of individual ChB contributions while minimizing the influence from the contribution of pure and non-directional ion-pair Coulombic effects.

These interaction energies (indicated in red in Figure S 27) confirm that the bifurcated Ch,Ch···O ChBs are the strongest stabilizing interactions in compounds **1**–**4**. In these compounds, the oxygen acceptor is located in the middle of a Ch–Ch bond on the molecular plane, which aligns with the high positive potential regions identified in the MEP surface analysis. The energies for these dominant bifurcated bonds are -9.4 kcal/mol in compound **4**, -7.6 kcal/mol in compound **3**, -7.8 kcal/mol in compound **2** and -6.1 kcal/mol in compound **1**. The increased energy for the $[Te_4]^{2+}$ compound does not align with the identified decreased positive MEP but in general fits into the expectation for an increased polarization for the heavier atoms compared to $[Se_4]^{2+}$,as well as the decreased HOMO-LUMO gap

reported within the literature.[41] Additionally, although a decreased Lewis basicity and thus decreased cation···anion interactions would be expected for the $[HS_3O_{10}]^-$ compound (**3**) compared to **1**, the energies of the bifurcated bonds show the opposite. The observed short and very narrow O···Se distances within **2** and the high planarity of the respective cation are most likely caused by this increased energy. Interestingly, the ChB induced Te–Te bond elongation for the halidometalates $Te_4[SbF_6]_2$, and $Te_4[TaX_6]_2$ (X = Cl, Br) shows the same trend, whereby the less electronegative halogen (the weaker bases) show stronger cation···anion interactions.[42-43]

The energies of the additional, auxiliary Se···O and Te···O contacts in compounds **2** to **4** are a unique feature of the longer-chained (hydrogen-)polysulfates. They are very small (–0.7 to –1.5 kcal/mol), indicating they play only a minor role and are not structure-directing.

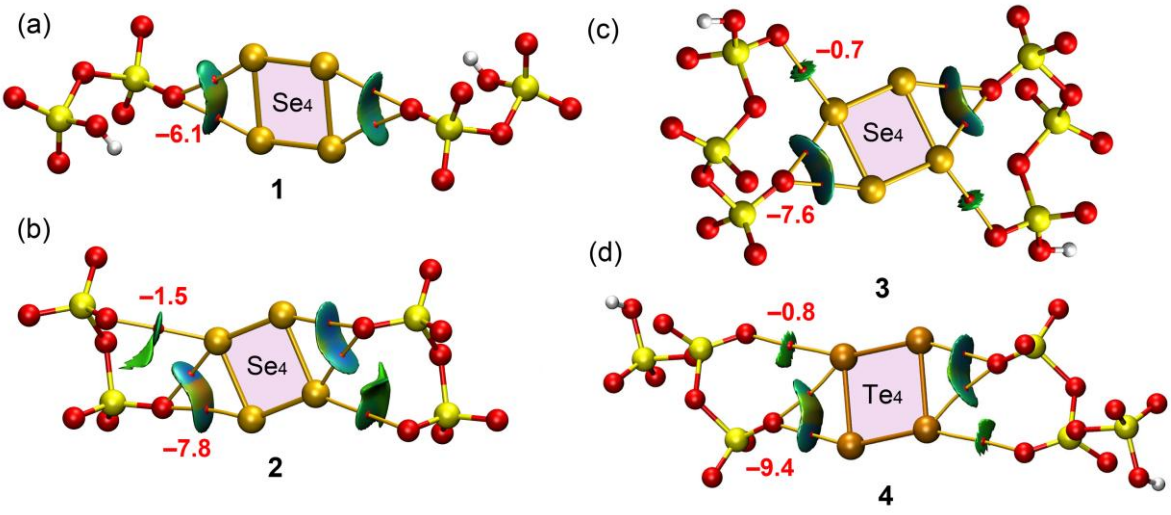

Figure S 27: QTAIM/NCIplot analyses of the Ch··· O ChBs in trimeric assemblies of **1** (a), **2** (b) and **3** (c) and **4** (d). Small red spheres represent BCPs, interconnected by orange bond paths. The green/blue isosurfaces indicate weak to moderate attractive non-covalent interactions (NCI). Interaction energies (in kcal/mol) calculated via an energy predictor based on the QTAIM potential energy density (V) are shown in red.

The crystal packing of compound **4** presents a more complex scenario (see Figure S 28), with three anions located around the $[Te_6]^{4+}$ cation, interacting with the three rectangular faces of the trigonal prism. The first anion is connected by two BCPs via a strong bifurcated Te,Te···O ChB (–6.5 kcal/mol). The respective RDG isosurface spans the entire rectangular face, indicating collective participation in the interaction. This aligns with the absolute maximum potential ($V_{S,max}$) identified at the center of the square faces. The second anion forms a combination of three ChBs: a weaker bifurcated Te,Te···O ChB (–2.0 kcal/mol) and a moderately strong individual Te···O ChB (–3.1 kcal/mol). The third anion contributes the greatest stabilization, connected by three individual Te···O ChBs resulting in a remarkably high total combined energy of –14.3 kcal/mol. This dense and strong combination of interactions perfectly aligns with the large positive potential observed on the rectangular faces of the Te64+ prism in the MEP analysis. The energy of the already mentioned auxiliary Te···O contacts (i.e.

coordination by oxygen atoms within the polysulfate chain, which usually have strongly decreased oxoanionic character) is strongly increased for the $[Te_6]^{4+}$ compounds.

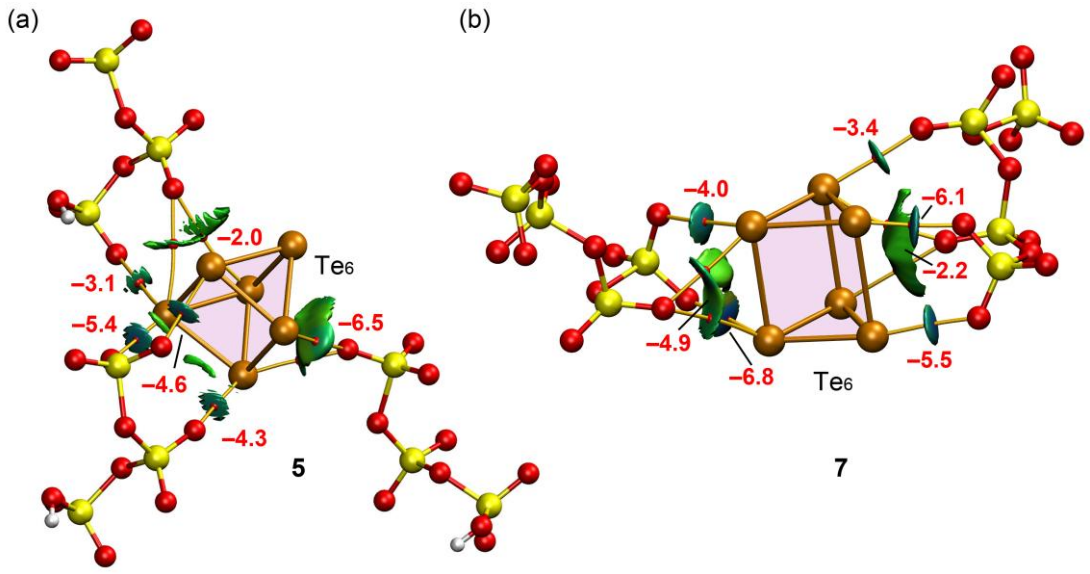

Figure S 28: QTAIM/NCIplot analyses of the Te··· O ChBs in tetrameric assemblies of **5** (a) and trimeric assembly of **7** (b). Small red spheres represent BCPs, interconnected by orange bond paths. The green/blue isosurfaces indicate weak to moderate attractive non-covalent interactions (NCI). Interaction energies (in kcal/mol) calculated via an energy predictor based on the QTAIM potential energy density (V) are shown in red.

Compound **7**, conversely, features a predominant interaction involving two anions and the rectangular faces. The first of these two anions forms four ChBs, comprising a bifurcated Te,Te···O ChB (– 4.9 kcal/mol) alongside two notably strong individual Te···O ChBs (–4.0 and –6.8 kcal/mol). The second anion exhibits an even higher coordination number, forming five ChBs, which consist of one bifurcated Te,Te···O ChB (–2.2 kcal/mol) and three individual Te···O ChBs ranging in strength from – 3.4 to –6.1 kcal/mol.

Finally, we also analyzed π-hole ChBs in compound **1**, which are represented in Figure S 29. As suggested by the MEP analysis, the $[Se_4]^{2+}$ dication presents two π-holes located above and below the molecular plane. The QTAIM analysis confirms this interaction: one oxygen atom of each anion is connected to one of the Se atoms of the square by a BCP and bond path, with an estimated interaction energy of -1.2 kcal/mol. The π-hole nature of this ChB is visibly represented by the RDG isosurface (green in Fig. S 29a) that embraces most of the $[Se_4]^{2+}$ square ring. Furthermore, the NBO analysis (Fig. S29b) supports this finding by showing an electron donation from the LP orbital at the closest oxygen atom of the anion to the π* antibonding Se–Se orbital (LP(O) → π*(Se–Se)). Although the calculated stabilization energy (1.0 kcal/mol) is modest compared to the σ-hole interactions described previously, it is crucial as it reveals the duality of $[Se_4]^{2+}$ to participate in both σ-hole and π-hole non-covalent interactions.

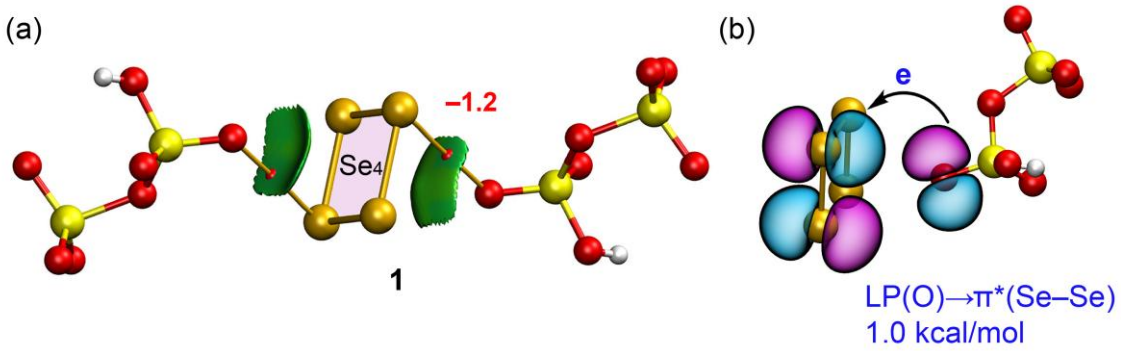

Figure S 29: Analysis of π-Hole Chalcogen Bonding in Compound **1**. (a) QTAIM/NCIplot analysis illustrating the π-hole interaction. (b) NBO analysis confirming the orbital contribution from the LP(O) → π*(Se–Se) charge transfer, with a stabilization energy of 1.0 kcal/mol.

References

[1] G. Brauer, *Handbuch der Präparativen Anorganischen Chemie*, 3 ed., Ferdinand Enke Verlag, Stuttgart, **1975**.
[2] R. King, S. Sangokoya, *Inorg. Chem.* **1987**, *26*, 2727-2730.
[3] I. D. Brown, D. B. Crump, R. J. Gillespie, *Inorg. Chem.* **1971**, *10*, 2319-2323.
[4] J. Langwald, L. Ebels, M. Symeonidis, J. Bruns, A. Frontera, M. S. Wickleder, *unpublished work*.
[5] C. Logemann, J. Bruns, L. V. Schindler, V. Zimmermann, M. S. Wickleder, *Z. Anorg. Allg. Chem.* **2015**, *641*, 831-837.
[6] Bruker AXS, *APEX 5 v2023.9-2* **2023**, Madsion, Winconsin, USA.
[7] SmartLabStudioII, *Rigaku Corporation* **2014**, Version 4.4.295.290.
[8] L. Krause, R. Herbst-Irmer, G. M. Sheldrick, D. Stalke, *J. Appl. Crystallogr.* **2015**, *48*, 3-10.
[9] O. V. Dolomanov, L. J. Bourhis, R. J. Gildea, J. A. K. Howard, H. Puschmann, *J. Appl. Crystallogr.* **2009**, *42*, 339-341.
[10] G. Sheldrick, *Acta Crystallogr. Sect. A: Found. Crystallogr.* **2015**, *71*, 3-8.
[11] G. Sheldrick, *Acta Cryst. Sect. C* **2015**, *71*, 3-8.
[12] Crystal Impact GbR, *Diamond 4.6.8* **2022**, Bonn, Germany.
[13] A. Coelho, *TOPAS 64, Version 6* **2016**.
[14] A. Coelho, *J. Appl. Crystallogr.* **2018**, *51*, 210-218.
[15] P. Thompson, D. E. Cox, J. B. Hastings, *J. Appl. Crystallogr.* **1987**, *20*, 79-83.
[16] J. Langwald, R. M. Gomila, D. van Gerven, A. Frontera, M. S. Wickleder, *Dalton Trans.* **2025**, *54*, 16095-16105.
[17] J. Bruns, C. Kolb, M. S. Wickleder, *Z. Anorg. Allg. Chem.* **2014**, *640*, 2345.
[18] C. Logemann, T. Klüner, M. S. Wickleder, *Angew. Chem. Int. Ed.* **2012**, *51*, 4997-5000.
[19] L. Link, R. Niewa, *J. Appl. Crystallogr.* **2023**, *56*, 1855-1864.
[20] J. Bruns, O. Niehaus, R. Pöttgen, M. S. Wickleder, *Chem. Eur. J.* **2014**, *20*, 811-814.
[21] L. V. Schindler, M. Daub, M. Struckmann, A. Weiz, H. Hillebrecht, M. S. Wickleder, *Z. Anorg. Allg. Chem.* **2015**, *641*, 2604-2609.
[22] L. V. Schindler, T. Klüner, M. S. Wickleder, *Chem. Eur. J.* **2016**, *22*, 13865-13870.
[23] Renishaw plc., *WiRE 5.1* **2017**, New Mills, UK.
[24] OriginLab Corporation, *OriginPro, Version 2024* **2024**, Northampton, MA, USA.
[25] R. J. Gillespie, G. P. Pez, *Inorg. Chem.* **1969**, *8*, 1229-1233.
[26] J. Bruns, T. Klüner, M. S. Wickleder, *Chemistry – An Asian Journal* **2014**, *9*, 1594-1600.
[27] A. Simon, H. Wagner, *Z. Anorg. Allg. Chem.* **1961**, *311*, 102-109.
[28] V. Varma, N. Rangavittal, C. N. R. Rao, *J. Solid State Chem.* **1993**, *106*, 164-173.
[29] R. C. Burns, R. J. Gillespie, *Inorg. Chem.* **1982**, *21*, 3877-3886.
[30] S. G. Balasubramani, G. P. Chen, S. Coriani, M. Diedenhofen, M. S. Frank, Y. J. Franzke, F. Furche, R. Grotjahn, M. E. Harding, C. Hättig, A. Hellweg, B. Helmich-Paris, C. Holzer, U. Huniar, M. Kaupp, A. Marefat Khah, S. Karbalaei Khani, T. Müller, F. Mack, B. D. Nguyen, S. M. Parker, E. Perlt, D. Rappoport, K. Reiter, S. Roy, M. Rückert, G. Schmitz, M. Sierka, E. Tapavicza, D. P. Tew, C. van Wüllen, V. K. Voora, F. Weigend, A. Wodyński, J. M. Yu, *J. Chem. Phys.* **2020**, *152*.
[31] E. D. Glendening, C. R. Landis, F. Weinhold, *J. Comput. Chem.* **2019**, *40*, 2234-2241.
[32] M. e. Frisch, G. Trucks, H. B. Schlegel, G. Scuseria, M. Robb, J. Cheeseman, G. Scalmani, V. Barone, G. Petersson, H. Nakatsuji, Gaussian, Inc. Wallingford, CT, **2016**.
[33] C. Adamo, V. Barone, *J. Chem. Phys.* **1999**, *110*, 6158-6170.
[34] E. Caldeweyher, C. Bannwarth, S. Grimme, *J. Chem. Phys.* **2017**, *147*.
[35] F. Weigend, R. Ahlrichs, *Phys. Chem. Chem. Phys.* **2005**, *7*, 3297-3305.
[36] F. Weigend, *Phys. Chem. Chem. Phys.* **2006**, *8*, 1057-1065.
[37] R. F. W. Bader, *Acc. Chem. Res.* **1985**, *18*, 9-15.
[38] J. Contreras-García, E. R. Johnson, S. Keinan, R. Chaudret, J.-P. Piquemal, D. N. Beratan, W. Yang, *J. Chem. Theory Comput.* **2011**, *7*, 625-632.
[39] T. Lu, F. Chen, *J. Comput. Chem.* **2012**, *33*, 580-592.
[40] A. Bauzá, A. Frontera, *ChemPhysChem* **2020**, *21*, 26-31.
[41] K. Tanaka, T. Yamabe, H. Teramae, K. Fukui, *Inorg. Chem.* **1979**, *18*, 3591-3595.

[42] J. Beck, G. Bock, *Z. Naturforsch. B* **1996**, *51*, 119-126.
[43] G. Cardinal, R. J. Gillespie, J. F. Sawyer, J. E. Vekris, *J. Chem. Soc., Dalton Trans.* **1982**, 765-779.